




Chair of Reservoir Engineering

Master's Thesis



Analytical and Numerical Analysis of the
Waterflood Performance of a Libyan Oil Field

Nina Romich, BSc

September 2019

Nina Romich, BSc.

Master Thesis 2019

Supervisor: Prof. Holger Ott, Dr. Barbara Male-Pirker

Analytical and Numerical Analysis of the Waterflood Performance of a Libyan Oil Field



EIDESSTATTLICHE ERKLÄRUNG

Ich erkläre an Eides statt, dass ich diese Arbeit selbständig verfasst, andere als die angegebenen Quellen und Hilfsmittel nicht benutzt, und mich auch sonst keiner unerlaubten Hilfsmittel bedient habe.

Ich erkläre, dass ich die Richtlinien des Senats der Montanuniversität Leoben zu "Gute wissenschaftliche Praxis" gelesen, verstanden und befolgt habe.

Weiters erkläre ich, dass die elektronische und gedruckte Version der eingereichten wissenschaftlichen Abschlussarbeit formal und inhaltlich identisch sind.

Datum 09.09.2019

A handwritten signature in blue ink that reads 'Nina Romich'.

Unterschrift Verfasser/in
Nina, Romich
Matrikelnummer: 01435350

Acknowledgements

I would like to show my appreciation and gratitude for the help and support to following persons who have contributed in making this thesis possible.

First, I would like to thank my supervisor, Dr. Barbara Male-Pirker for her expertise, guidance and support. This includes the careful reading of this thesis and especially her dedication to teach me valuable know-how whenever I had questions.

My sincere thanks also go to Prof. Dr. Holger Ott, for the continuous support, for his motivation, and immense knowledge. I would like to thank you very much for your expertise and understanding over these past five years in university.

Furthermore I want to thank DI Pit Arnold and DI Anthony Simpkins for their advices and valuable input. I highly appreciate that they always had a sympathetic ear whenever I needed support.

Finally, I must express my very profound gratitude to my family and to my partner for providing me with unfailing support throughout my years of study and through the process of writing this thesis. This accomplishment would not have been possible without them.

Abstract

This thesis supports the re-development work of a Libyan oil field in the Sirte Basin, which is producing since 1966. Pressure decreased rapidly after production was started, therefore a line-drive waterflooding scheme was implemented in the early 1970s to provide pressure support. Within the next few years, a re-development will take place to improve the sweep of the waterflood, as there are some areas of the field, where the production performance is insufficient. The objective is to analyze the injection scheme and recommend modifications to improve the flood efficiency. Finally, possible drilling locations for new injection and production wells should be provided to significantly enhance the oil recovery. The suggested re-development actions should be underpinned by an economic evaluation.

To gain a first insight and indications analytical analysis were performed. Pressure, water-oil-ratio, water cut, areal and vertical sweep efficiency calculations and a Buckley-Leverett-calculation were conducted.

Afterwards material balance calculations were performed using MBAL, regarding the results of the analytical methods. A MBAL-model was built in a way that it is able to reproduce historical behavior of the field in a sufficient way. Based on the analytical pressure analysis and the MBAL model three pressure regions were identified that show characteristic pressure trends: “Low”, “High” and “Increasing”.

To further transfer those results into a numerical model, simple box models were created using PETREL. The locations of those blocks within the field were chosen such, that each block represents one pressure region. To optimize the waterflood performance, simulations on the blocks were performed using ECLIPSE with different pattern configurations. The additional recovery was evaluated to find an optimum well arrangement with the most favorable spacing and to decide whether or not to modify the injection scheme.

It was determined that two regions of the field should be converted to a 5-spot-pattern flood instead of the currently installed line drive. Cumulative oil production could be enhanced significantly by re-arranging the injector/producer setting.

Zusammenfassung

Diese Diplomarbeit unterstützt die Arbeit rund um das Re-Development eines libyschen Ölfelds im Sirte Becken, welches seit dem Jahr 1966 produziert. Aufgrund rapider Druckverluste in den ersten Produktionsjahren wurde ein Line-Drive Wasserflutungsschema in den 1970er Jahren implementiert um den Lagerstättendruck zu unterstützen. In den nächsten Jahren wird ein Re-Development des Ölfelds stattfinden um die Effizienz der Wasserflutung zu steigern, da bestimmte Regionen innerhalb des Feldes eine unzureichende Produktionsleistung aufweisen. Ziel ist es, das derzeitige Injektionsschema zu analysieren und Verbesserungsvorschläge zu machen um die Flutungseffizienz zu steigern. Es sollten Standorte für neue Bohrungen von Injektoren und Produzenten festgelegt werden um die Ölförderung maßgeblich zu steigern. Diese Sanierungsvorschläge sollten durch eine wirtschaftliche Analyse untermauert werden.

Um einen ersten Einblick zu erlangen wurden analytische Berechnungen durchgeführt. Druck, Wasser-Öl-Relationen und die volumetrische Flutungseffizienz wurden analysiert. Außerdem wurde eine Buckley-Leverett-Berechnung durchgeführt. Mit den Ergebnissen der analytischen Berechnung wurde eine Materialbilanz mit MBAL berechnet. Ein MBAL-Modell wurde erstellt, welches das historische Verhalten der Lagerstätte zu einem ausreichenden Grad nachbilden konnte. Aufgrund dieser Ergebnisse wurden drei Druckregionen identifiziert („Low“, „High“ und „Increasing“), welche vergleichbares Druckverhalten in den letzten Jahren aufweisen. Um diese Ergebnisse in ein numerisches Modell zu transferieren wurden einfache Box Modelle in PETREL gebildet. Die Lage dieser Blöcke innerhalb des Ölfelds wurde so gewählt, dass jeder Block eine der drei Druckregionen repräsentiert. Um die Performance der Wasserflutung zu optimieren wurden Simulationen mit diesen Blöcken mit verschiedenen Flutungsmustern in ECLIPSE ausgeführt. Die erhöhte Rückgewinnungsrate wurde evaluiert um eine optimale Anordnung der neuen Bohrungen mit dem bestmöglichen Abstand zueinander zu finden und um zu zeigen, ob eine Modifikation des Injektionsschemas sinnvoll ist. Es wurde festgestellt, dass zwei der drei Regionen von einem Line-Drive-Schema zu einem 5-Spot-Muster konvertiert werden sollten. Durch die neue Anordnung von Injektoren und Produzenten könnte die kumulative Ölproduktion in den entsprechenden Regionen maßgeblich verbessert werden.

Table of Contents

Chapter 1	Introduction.....	13
1.1	Background and Context.....	14
1.2	Scope and Objectives	15
1.3	Achievements.....	15
Chapter 2	Literature Review.....	17
2.1	Basic Concepts.....	17
2.2	Reservoir Management for Waterfloods	24
2.3	Analytical Methods to Predict Waterflood Performance	28
2.4	Numerical Methods to Predict Waterflood Performance	32
2.5	Extension of Waterflooding.....	33
Chapter 3	Analytical Analysis.....	37
3.1	Pressure Analysis	38
3.2	WOR Analysis	40
3.3	Water Cut Analysis	42
3.4	Determination of Volumetric Sweep Efficiency	42
3.5	Determination of Areal Sweep Efficiency	44
3.6	Buckley Leverett Frontal Advance Theory.....	44
3.7	Material Balance Calculation.....	47
Chapter 4	Numerical Analysis.....	55
4.1	Block: Low.....	58
4.2	Block: High	60
4.3	Block: Increasing	64
4.4	Sector Models.....	67
Chapter 5	Results and Discussion.....	75
5.1	Economic Evaluation Pressure Region “High”.....	75
5.2	Economic Evaluation Pressure Region “Increasing”	77
Chapter 6	Conclusion.....	79
6.1	Summary	79
6.2	Evaluation	80
6.3	Future Work	81
Chapter 7	References.....	83

Chapter 1

Introduction

Typically more than 80% of the original oil in place is left behind using only primary recovery mechanisms like solution gas drive or liquid and rock expansion. (Bradley, 1987) Waterflooding is the most important method for improving recovery from oil reservoirs and belongs per definition to secondary recovery mechanisms. Water is injected into a reservoir to induce a viscous drive towards the producing well and maintain or increase the reservoir pressure. Billions of barrels have been additionally recovered worldwide by waterflooding after the economically productive limit of primary recovery methods was reached.

The success of a waterflood process is mainly dependent on proper reservoir management practices, which include designs based on accurate relative permeability data and an optimum injector/producer array that takes local crustal stress directions in the reservoir into account. Increasing oil production and ultimately oil recovery as well as maintaining the pressure above bubble point to avoid gas breakout is crucial for maintaining high well productivity. (Bradley, 1987) (Thakur, 1998)

This thesis deals with the evaluation of the waterflood efficiency of a Libyan oil reservoir (see Figure 1). Analytical analysis of pressure and production data as well as numerical simulations for selected regions of the field are performed to give indications for a flood pattern optimization.

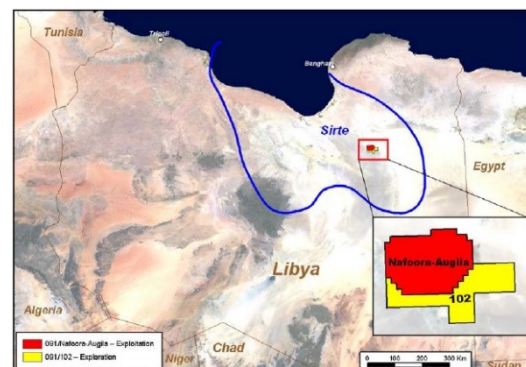


Figure 1: Index map (OMV, 2008)

1.1 Background and Context

The oil field of interest is located in the Sirte Basin in Libya and has been producing since 1966. The reservoir is highly heterogeneous and extends over a limestone unit, a sandstone unit and a granite basement (See Figure 2).

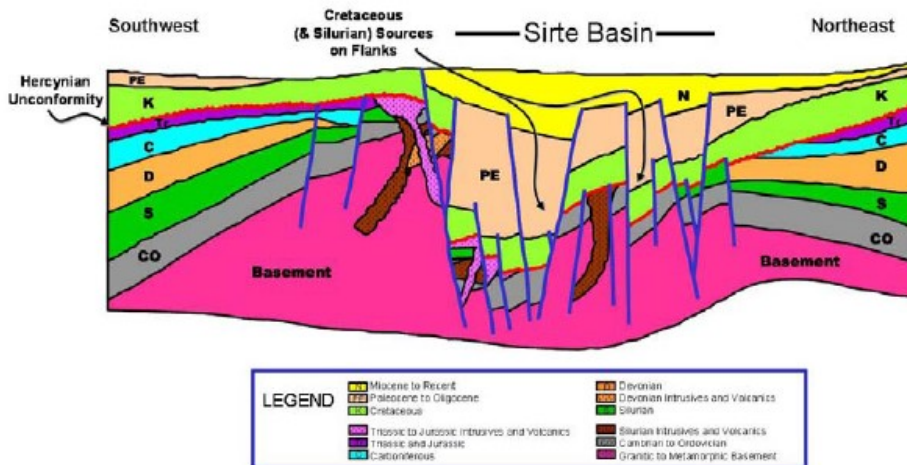


Figure 2: Cross section across Sirte Basin (OMV, 2008)

The limestone is subdivided into 5 major units: top layers D and E, which are quite tight and F, G and H layers with a good permeability and good reservoir properties. (See Figure 3)

The estimated oil initially in place is 5.5 BSTB. It is a typical black oil reservoir with low GOR and low oil viscosity. This makes the reservoir a good candidate for water flooding. (Lake, 2007) (Dake, 1978)

Peak production was reached in 1969 at almost 350,000 BOPD. Aquifer support in the early years of production seems to be negligible as the pressure decreased rapidly with production. In the early 1970s a line-drive waterflooding scheme was implemented to provide pressure support. Currently the water cut of the

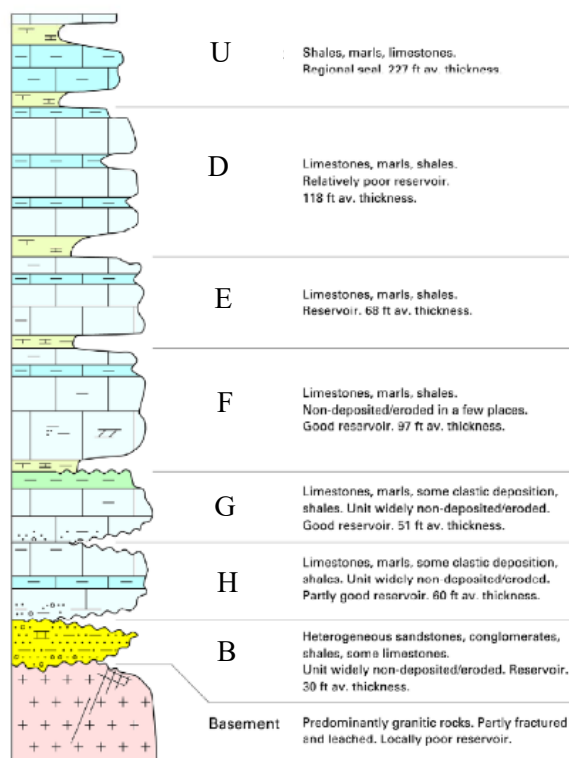


Figure 3: Lithostratigraphic Column (Muchitsch & Kratzer, 2005)

field is at approximately 60%. Well spacing is quite large which reveals potential for in-fill wells. A re-development plan focusing on improving the sweep efficiency of the waterflood is currently under progress.

1.2 Scope and Objectives

The scope of this thesis is to analyze the efficiency of the waterflood on different scales and to determine whether the injection scheme shows positive results or if modifications during the re-development of the field are reasonable to improve the waterflood efficiency. For this reason analytical analysis of the waterflood performance were conducted. Furthermore those analytical results are transferred into a 1D material balance model and into a numerical model by using a simple simulation model (box model) and full field simulations. The objective is to choose locations within the field that represent different areas with good and bad performance and to set up block models to optimize waterflood performance. A look is taken on the feasibility of optimizing the flood pattern and evaluating the additional recovery that could be achieved.

1.3 Achievements

During the analytical analysis of the field three different pressure regions could be identified. They were divided according to their pressure trends into 3 pressure regions: “High”, “Low” and “Increasing”. The water-oil-ratio and water cut analysis further revealed regions with potential for improvement. Using simple box models it was possible, to evaluate the performance of the currently installed line-drive waterflooding scheme and to identify regions where modifications should be done. Different patterns with altered spacings were applied to homogeneous blocks, which were built with averaged properties (permeability, porosity and water saturation) according to their position in the field. Finally, the results were applied to the whole sector including reservoir heterogeneity (=pressure region) for the regions with “High” and “Increasing” pressure trend. Based on those results recommendations for locations of new infill producers and injectors are given. The cumulative oil production of these two sectors could be improved significantly from about 240 MMSTB to 360 MMSTB with 47 new infill wells until the anticipated end of field life in 2045. Finally an economic evaluation was performed to emphasize the feasibility of the recommended re-development. The additional cashflow discounted to 2019 that could be generated with the new infill wells results in 1.4 BUSD.

Chapter 2

Literature Review

Waterflooding is accepted worldwide as a reliable and economically attractive recovery technique. Almost every significant oil field without a natural water drive is considered for waterflooding operations. The US was the pioneer in developing water injection operations and improving waterflood efficiency. Literature reports the first waterflooding operations in 1880 in Pithole City and in the 1890's in New York and Pennsylvania. (Bradley, 1987)

The main reason to perform waterfloods is to maintain or increase the reservoir pressure, supplement natural water influx and displace oil towards production wells. General availability of water, comparably low costs and high efficiency led to the circumstance that water flooding is the most common secondary recovery mechanism. (Craig, 1971)

2.1 Basic Concepts

This chapter deals with the basic concepts and terms that are used for waterflooding operations.

2.1.1 Mobility Ratio Concept

The concept of mobility (λ) was first introduced by Muskat (Muskat, 1951) and represents the ratio of effective permeability of the fluid (absolute permeability K multiplied with the relative permeability k_{ri} of the fluid) to the fluid viscosity (μ_i) and is a strong function of fluid saturation. It is calculated as follows:

$$\lambda_i = \frac{Kk_{ri}}{\mu_i}$$

The mobility ratio M describes the ratio of mobility of the displacing fluid to the mobility of the displaced fluid. Considering the case that water and oil is present, water is the displacing phase meanwhile oil is the displaced phase, therefore the denotations w and o are respectively used:

$$M = \frac{\lambda_{displacing}}{\lambda_{displaced}} = \frac{\lambda_w}{\lambda_o} = \frac{k_{rw} \mu_o}{\mu_w k_{ro}}$$

A mobility ratio below 1 is favorable as it leads to a stable, piston-like displacement. If the mobility ratio is higher than 1 the displacement is unfavorable, because it is unstable and viscous fingers are very likely to develop. In other words, if the displacing fluid has a tendency to move faster than the displaced fluid, the interface is unstable. Additionally, heterogeneity of the formation fosters the development of unstable displacement fronts. As a consequence, breakthrough of water occurs much faster, which apparently leads to a decreased recovery efficiency. (Muskat, 1951)

The mobility ratio influences the injectivity variation (injectivity = injection rate per unit pressure difference between the injection and production wells, (Deppe, 1961)) of a well as soon as the gas space is filled up. In Figure 4 the early period of injection corresponds to fillup of gas space and leads to a rapid decline of the injectivity at the beginning. Nevertheless, the much more important behavior is observed after that initial period. For a favorable mobility ratio below 1 the injectivity decreases with an increasing flood-front radius. For an unfavorable mobility ratio of higher than 1 the injectivity gradually increases.

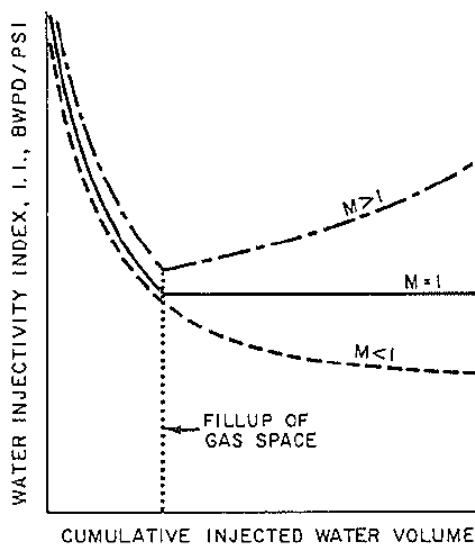


Figure 4: Water injectivity variation (Craig, 1971)

2.1.2 Volumetric Sweep Efficiency

Estimating volumetric sweep efficiency is highly important for mature waterfloods to determine the fraction of the reservoir which has been swept or not by the injected water and to find out if there is an additional oil recovery potential. It is a major goal of the waterflood management process to maximize the volumetric sweep efficiency from the beginning on. Computing volumetric sweep efficiency of the injected water is useful for the management and calculation of future waterflood recovery potential. (Cobb & Marek, 1997) (Thakur, 1998)

There are commonly two scales of waterflooding distinguished, which are namely microscopic and macroscopic scale. For microscopic scale the process in the porous network is of importance. Interactions between injected and in place fluids should be investigated by performing lab experiments for fluid fluid as well as for fluid rock interactions. For the macroscopic point the microscopic behavior is upscaled and structural set-ups and geological heterogeneities need to be taken into account as these features seriously impact the flow behavior. Pilots are necessary to validate extrapolation of microscopic scale results. It is of high importance to understand the physics and the influencing factors behind a fluid flow within a porous media to capture all forces that act on a fluid in a porous medium and furthermore reservoir conditions that might lead to oil entrapment.

The efficiency of a displacement process depends on microscopic and macroscopic displacement efficiency:

$$E = E_V * E_D$$

E .. overall displacement efficiency

E_V .. volumetric sweep efficiency / macroscopic displacement efficiency (heterogeneous)

E_D .. displacement efficiency / microscopic displacement efficiency (homogeneous)

$$E_D = \frac{\text{reservoir volume of oil mobilized}}{\text{reservoir volume of oil contacted}}$$

The microscopic displacement is related to the displacement of oil at pore scale and therefore is an indicator of the effectiveness of the displacing fluid to mobilize the oil, but only at those places where the displacing fluid contacts the oil.

Whereas the macroscopic displacement efficiency is related to the effectiveness of the displacing fluid to contact the reservoir in a volumetric sense. So it measures how effective the displacing fluid sweeps out the reservoir volume. (Buckley & Leverett, 1942) (Welge, 1952)

$$E_V = \frac{\text{reservoir volume of oil contacted by displacing agent}}{\text{reservoir volume of oil originally in place}}$$

Macroscopic displacement efficiency is a product of E_A and E_L :

$$E_A = \frac{\text{Area contacted by displacing agent}}{\text{Total area}}$$

$$E_L = \frac{\text{Length contacted by displacing agent}}{\text{Total vertical length}}$$

Volumetric sweep efficiency and displacement efficiency are necessary input values for the computation of cumulative oil recovery:

$$N_p = \frac{E_v E_D S_{oi} V_p}{B_o}$$

S_{oi} .. initial oil saturation

V_p .. pore volume

2.1.2.1 Areal Sweep Efficiency

Areal sweep efficiency calculations were developed to analytically find an optimum pattern that maximizes the contact of injection fluid with the oil. Several empirical methods are available to determine areal sweep efficiency. In general, areal sweep efficiency is dependent on (Craig, 1971):

- Well pattern
- Permeability heterogeneity
- Mobility ratio
- Relative importance of capillary, viscous and gravitational forces
- Volume of fluid injected

The most important factor is by far the mobility ratio. For mobility ratios below 1, areal sweep efficiency is generally high. The well pattern should be selected in a way that a linear flow is approached. Furthermore the different production stages before, at and after breakthrough have to be considered to determine areal sweep efficiency.

Several models exist to evaluate areal sweep efficiencies. All models depend on the analogy between Darcy's law and Ohm's law for a conductive medium that represents the reservoir geometry. (Bradley, 1987) For the computation at breakthrough Craig et. Al or Willhite Mathematical Representation of Craig Model can be applied. At or after breakthrough Dyes et al, Fassihi Representation of Dyes et. Al Model or Cuddle and Witte can be used.

2.1.2.2 Vertical Sweep Efficiency

Vertical sweep efficiency describes the ratio between the pore space invaded by the injected fluid to the pore space enclosed in all layers behind the location of the leading edge of the front.

In general the degree of heterogeneity is much more significant in vertical direction than in horizontal direction. An injection fluid will always seek the path of least resistance to flow and layers in the more permeable zones will be penetrated much faster. Areal and vertical sweep efficiency need to be combined appropriately to determine overall volumetric displacement efficiency. Nevertheless, factors need to be examined separately beforehand. Vertical Sweep efficiency is mainly dependent on:

- Heterogeneity
- Gravity effect (density differences)
- Mobility ratio
- Vertical to horizontal permeability
- Capillary forces

To determine vertical sweep efficiency correlations that consider gravity segregation effect (Craig, 1971) or correlations that consider reservoir heterogeneity (Dykstra & Parsons, 1950) are available.

2.1.3 Waterflooding Patterns

The goal of selecting a certain geometric pattern is to form a symmetrical and interconnective network over a large areal extent. Bypassed oil in undrained compartments wants to be minimized. Generally it has to be outlined that larger volumes of water lead to significantly higher producing rates and horizontal water injection enhances injection rates and injection pressures considerably.

Numerous different injection/production well patterns have been used. The most common ones are direct line drive, staggered line drive, five-spot, seven-spot and nine-spot. (Muskat, 1951) (Kimbler, et al., 1964) Different pattern configurations are shown in Figure 5 (Rose, et al., 1989). As visible, the direct line drive involves injectors and producers on a direct line, whereas the staggered line drive involves staggered injectors and producers. Four-, five-, seven- and nine-spot patterns include either injectors at the corners and a producer at the center (regular) or producers at the corners and an injector at the center (inverted). (Rose, et al., 1989)

Overall, well arrangements are typically irregular, peripheral, regular or crestal and basal injection pattern. Furthermore, horizontal water injection can significantly enhance injection rates and injection pressures. Much without fracture stimulation are possible. (Kimblor, et al., 1964)

The flood pattern selection is one of the first steps in designing a waterflood project and influences volumetric sweep efficiency substantially. Literature reports sweep efficiencies of 72 per cent for five-spot patterns, 56 per cent for line drive patterns and a range of 45 to 90 per cent for the nine-spot pattern (under the assumption of homogeneous reservoirs, steady-state conditions, negligible gravity and capillary effects). (Crawford, 1960)

Reaching the maximum possible contact of the injection fluid with the crude oil system is the major objective during the pattern selection. Reservoir heterogeneity, directional permeability, direction of formation fractures, availability of the injection fluid, maximum oil recovery, flood life, well spacing, productivity and injectivity influence the selection of the most appropriate pattern.

Nevertheless, designing waterflood operation corresponding to one of the standard geometrical flood patterns is often not appropriate or even not possible.

2.1.4 Injection Rates

Oil recovery and subsequently the life of a waterflood depends mainly on the water injection rate into a reservoir. Many factors influence the rate of injection and variations through the life of the project are common. The injection rates are affected by various parameters like rock and fluid properties, areas and fluid mobilities of the swept and unswept regions, pattern, spacing and wellbore radii. The water injectivity is defined as the injection rate per unit pressure difference between the injection and production wells. Deppe (Deppe, 1961) came up with

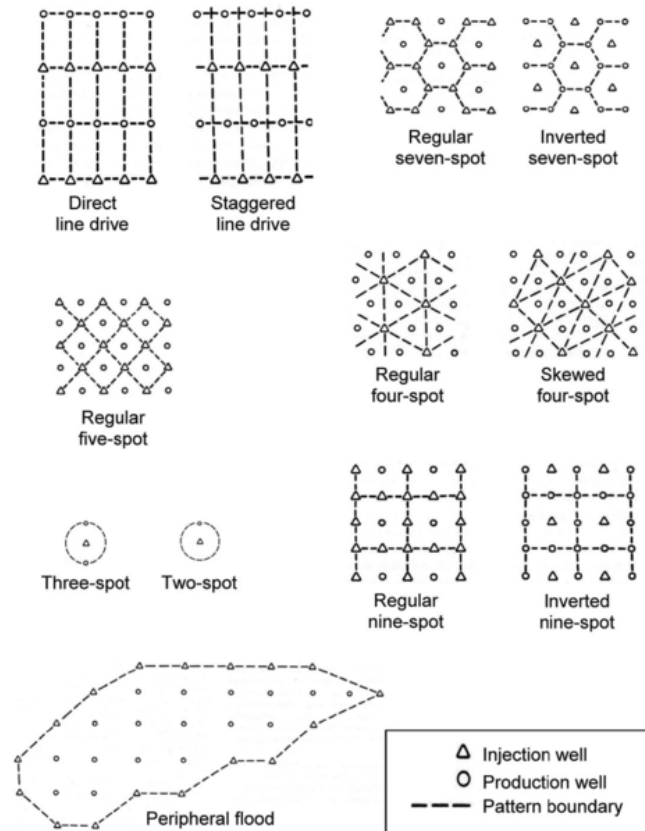


Figure 5: Common waterflood-pattern configurations (Rose, et al., 1989)

injection rate equations for regular patterns (assuming a constant mobility ratio of 1 and no free gas saturation) and Craig (Craig, 1971) summarized these equations. It has to be outlined that injectivity variation depends upon mobility ratio and increases unfavorably in case of a mobility ratio of higher than 1.

The injectivity for a direct line drive is: (Craig, 1971)

$$i = \frac{0.001538Kk_{ro}h\Delta P}{\mu_o \left(\log\left(\frac{a}{r_w}\right) + 0.682\frac{d}{a} - 0.798 \right)}$$

2.1.5 Voidage Replacement Ratio (VRR)

The voidage replacement ratio refers to the replaced volume of produced oil, gas and water from the reservoir by injected water. So, it is the ratio between reservoir barrels of injected fluid to reservoir barrels of produced fluid. Mathematically it can be expressed as:

$$VRR = \frac{\text{Injected reservoir volume [rbbl]}}{\text{Produced reservoir volume [rbbl]}} = \frac{B_w I_w}{B_o q_o + q_o B_g (GOR - R_s) + B_w q_w}$$

B_x .. formation volume factor for fluid type x

I_x .. injected volume for fluid type x

q_x .. produced volume for fluid type x

GOR.. produced Gas Oil Ratio

R_s .. solution Gas Oil Ratio

The voidage replacement ratio is calculated on an instantaneous basis. GORs have to be updated continuously based on instantaneous volumes. Also calculating a cumulative VRR with GORs calculated from cumulative fluids is quite common for the entire field. Figure 6 shows a possible outcome of instantaneous and cumulative VRR for a sample set of wells.

The value for the instantaneous VRR commonly starts with values higher than 1 for the first period of time. This goes along with the purpose of waterflooding that is enhancing recovery by maintaining reservoir pressure or even increasing reservoir pressure. If the instantaneous VRR would be lower than 1 the reservoir pressure declines. Cumulative VRR works the other way round, as the cumulative VRR reaches 1 it means that the reservoir pressure has been increased to near original reservoir pressure.

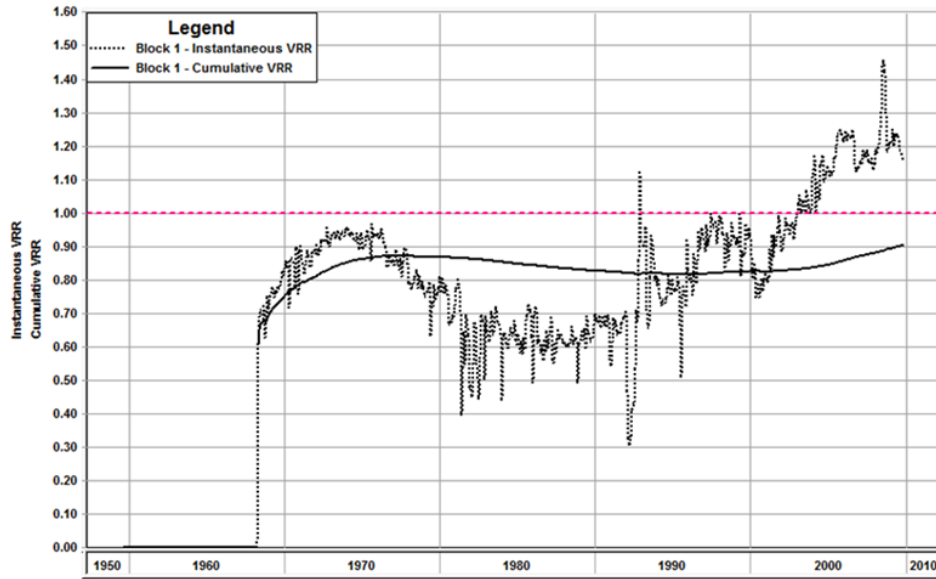


Figure 6: Instantaneous VRR and cumulative VRR for a sample set of wells (Anon., 2012)

The optimum voidage replacement ratio would be 1. Nevertheless, even if the VRR is maintained at 1 it does not always mean that the reservoir pressure is constant. If the material balance of fluids is conserved it does not automatically mean that also pressure is conserved. VRR should be tracked at the field level, reservoir, fault block and even by pattern. (Anon., 2012)

2.2 Reservoir Management for Waterfloods

Several steps are necessary to finally be able to make reasonable waterflooding efficiency predictions either analytically or numerically. A proper waterflood management should include information of reservoir characterization, pay areas containing recoverable oil, reservoir driving mechanisms and pattern performance analysis, data gathering, reservoir pressure monitoring and well information. In this chapter the most important reservoir management practices are described in more detail.

2.2.1 Reservoir Characterization

Reservoir engineers try to predict oil recovery performance by gathering all necessary basic data, evaluating and continuously updating these data to prepare a reasonable reservoir characterization. Special laboratory tests are requested like relative permeability or capillary pressure characteristics. Finally these data is utilized to investigate different flooding patterns, locations for injection and production wells, estimating injectivity and much more. (Craig, 1971)

In the waterflood designing procedure a proper reservoir characterization belongs to the crucial parts. Reservoir geometry, lithology, reservoir depth, porosity, permeability, continuity of reservoir rock properties, magnitude and distribution of fluid saturations, fluid properties, relative-permeability relationships and optimal time to waterflood should be determined (Bradley, 1987).

The **reservoir geometry**, namely structure and stratigraphy, controls the location of the wells. The presence and strength of a natural water drive is identified by analyzing reservoir geometry and past reservoir performance. In case of a strong natural water drive or highly faulted reservoirs water flooding operations might be economically unattractive.

Lithology factors which have to be taken into account are porosity, permeability and clay content. Clay minerals might lead to pore-clogging if they get in contact with water. Those effects should be evaluated in laboratory experiments.

Reservoir depth and accompanying fracture pressures further influence equipment selection and plant design. Also the number and location of injection wells is planned based on this restricting maximum pressure that can be applied. (Bradley, 1987)

Porosity influence is crucial for the total recovery, because it determines the amount of oil that is present for any given percent of oil saturation.

Permeability mainly controls the maximum rate/pressure of water injection that can be applied for an injection well taking the formation breakdown pressure into account.

Continuity strongly affects the suitability of a reservoir for waterflooding. Especially horizontal continuity is of primary interest as the fluid flow is essentially in direction of bedding planes.

In terms of **fluid properties** the viscosity of oil and subsequently the mobility ratio between displacing (water) and displaced (oil) fluid are important.

The **optimum time to start a waterflood** is dependent on the objective that wants to be met. Achieving maximum oil recovery, maximum future net income, stabilized rate etc. lead to different flooding strategies depending on which of the objectives is of primary concern. (Bradley, 1987)

Cole (Cole, 1969) listed important factors for determining the reservoir pressure or time to initiate a waterflood:

1. Reservoir Oil Viscosity
2. Free gas saturation
3. Cost of injection equipment

4. Productivity of producing wells
5. Effect of delaying investment on time value of money
6. Overall life of the reservoir

Regarding the oil viscosity the optimum time for the initialization would be when the pressure equals bubble point pressure as the viscosity of oil is at a minimum and consequently the oil mobility is at maximum which leads to a maximum sweep efficiency. The free gas saturation on the other hand should be at least 10%, which would only come up if pressure is below bubble point pressure. An immobile free gas saturation is beneficial in a water-wet system to reduce the residual oil saturation and furthermore increase the recovery, because pore space that would be occupied by residual oil droplets, is occupied by gas bubbles. (Feigl, 2011) The cost of injection equipment is apparently higher for higher reservoir pressures, but productivity is higher at higher pressures. Delaying the time of investment is desirable in terms of economics but regarding the overall life of the reservoir fluid injection should be started as soon as possible. (Cole, 1969) All those interacting factors need to be regarded and evaluated to determine the optimum time to start a waterflood.

2.2.2 Reservoir Driving Mechanisms

In case of strong water drive reservoirs is it usually not recommended to perform water flood operations. Nevertheless, there are some instances where water injection can be implemented, for example to support a higher withdrawal rate, increase uniform area coverage and better distribute water volume to different areas of the field or to balance voidage and influx volumes. Also gas cap drive reservoirs are commonly not optimal waterflood prospects as the primary recovery mechanism might be quite efficient anyway.

Optimum candidates for waterflooding interventions are generally solution gas drive reservoirs. For feasibility reasons waterflooding candidates should be in the best case shallow (less operating costs), have low energy oil (low GOR) and high permeability. (Dake, 1978)

2.2.3 Design and Management

Several parties and disciplines are involved in creating an effective design for waterflooding. A vast amount of information is required upfront, but also after initializing the waterflood several surveillance and monitoring techniques should be implemented to continuously update and improve the reservoir model and the applied techniques to reach the best possible recovery efficiency. Thakur et al pointed out the urgent need for an integrated technology development process and came up with different phases for the asset management process. Those phases can be summarized as follows (Thakur, 1998):

1. Framing waterflood opportunity

2. Consideration of alternatives
3. Development of preferred alternatives
4. Implementation of waterflood management plan
5. Operation, monitoring and evaluation of waterflood

Framing waterflood opportunity

During this step the business opportunity should be defined and key elements that impact the goal need to be evaluated. Furthermore reservoir and fluid characteristics are determined and also available technology as well as the estimated project life should be taken into account to develop a first description of the project and to conduct a rough economic analysis and determine the potential economic attractiveness of the project.

Consideration of alternatives

A first reservoir description including rock, fluid properties and fluid flow mechanisms with various development and depletion strategies is the main goal of this step. Based on this schedules for drilling and completion as well as facility requirements are estimated and project economics are evaluated. Finally the best alternatives based on the available data should be chosen to continue with the next step.

Development of preferred alternatives

A more detailed evaluation is now conducted that includes assumptions, methods used, screening criteria and guidelines for calculation of unknown parameters. Furthermore potential problems including causes and solutions should be outlined to perform risk analysis. Finally management and government approval is sought and a waterflood asset management plan is developed.

Implementation of waterflood management plan

During this step material and equipment needed should be designed, sized and selected. Also surface and subsurface facilities need to be fabricated, installed and tested, wells are drilled and completed and artificial lift or other field equipment is installed. Log, core and well test data is acquired and analyzed to upgrade the reservoir database. The waterflood operating plan and schedule is finalized and a surveillance and monitoring plan is developed including the selection of an operating team.

Operation, monitoring and evaluation

Monitoring and surveillance needs to be continued throughout the whole lifetime of the project. Production and injection rates of oil, gas and water, bottom hole pressure tests and records of workover and results are just examples of the vast amount of data that can and should be

collected for analysis. Performance monitoring of the reservoir, wells and facilities are a prerequisite for the modification and upgrade of the existing reservoir model. Plans and strategies need to be continuously revised and new expansion opportunities should be identified.

2.3 Analytical Methods to Predict Waterflood Performance

This chapter deals with analytical aspects of the displacement process analysis. Predicting future oil recovery and reservoir performance for a waterflood are the basis for defining the economic viability of a project. Predictions should be done for future well requirements and recompletions, well injection and producing rates, reservoir and injection pressures, producing WOR's and oil recovery. (Bradley, 1987)

2.3.1 Volumetric Method (Based on Material Balance)

The volumetric approach calculates the additional waterflood oil recovery based on the original oil in place prior to the waterflood and the recovery efficiency. The recovery efficiency factor is estimated based on the displacement efficiency (e.g. from laboratory flood tests) and an estimated volumetric sweep efficiency. If water-oil relative permeability curves are available, residual oil saturation and displacement efficiency can be estimated from fractional flow theory.

This approach is useful for the initial project screening, but it does not provide oil production rate vs. time performance and therefore is not suitable for economic evaluation of a waterflood project.

Estimation of the volume of oil that would be produced by waterflooding from a reservoir is done based on a simple material balance and only requires knowledge of the contacted fraction of reservoir volume by water (volumetric sweep efficiency) and the change in oil saturation in the water-contacted portion of the reservoir. The following equation can be applied to estimate the displaced oil from the swept parts of the reservoir:

$$N_d = \frac{E_v \Delta S_o V_p}{B_o}$$

N_d .. oil displaced from the swept parts of the reservoir

E_v .. volumetric sweep efficiency

ΔS_o .. change in average oil saturation in the swept parts of the reservoir

B_o .. formation volume factor for the oil

It has to be mentioned that this approach is only reasonable if there is zero gas saturation everywhere at the start, otherwise the displaced oil does not equal the produced oil through the production wells.

The material balance can be set-up as follows:

1. Volume of oil present at the end of primary production: $N-N_p$
2. After waterflooding: different oil saturations in un-swept and swept parts

$$\text{Oil in un-swept parts: } \frac{V_p(1-E_v) S_{oi}}{B_o}$$

$$\text{Pore volume can be related to initial oil in place: } N = \frac{V_p(S_{oi})}{B_{oi}} \text{ or } V_p = \frac{N B_{oi}}{S_{oi}}$$

$$\text{Therefore volume present in un-swept parts: } \frac{N(1-E_v)B_{oi}}{B_o}$$

3. Volume of oil present after waterflood in swept part: $\frac{V_p(E_v) S_{or}}{B_o} = \frac{N S_{or}(E_v)B_{oi}}{S_{oi}B_o}$

4. If those two parts are added the volume of remaining oil is given as:

$$\frac{N(1-E_v)B_{oi}}{B_o} + \frac{N S_{or}(E_v)B_{oi}}{S_{oi}B_o} = N \frac{B_{oi}}{B_o} \left((1-E_v) + E_v \frac{S_{or}}{S_{oi}} \right) = N \frac{B_{oi}}{B_o} \left(1 + E_v \left(\frac{S_{or}}{S_{oi}} - 1 \right) \right)$$

5. Now the volume of oil produced during a waterflood can be computed by calculating the difference between the oil present at the start and end of the waterflood. (Walsh, 1995)

2.3.2 Buckley Leverett Frontal Advance Calculation (Buckley & Leverett, 1942)

The frontal advance calculation is derived from the concept of fractional flow presented by Buckley and Leverett (Buckley & Leverett, 1942). Waterflooding is often considered as ideal immiscible displacement. Finite solubility of the different phases in each other and compressibility of the fluid phases is ignored (although injection water displaces reservoir water in a miscible way). The main mechanism that acts during a waterflood is pressure maintenance or pressure increase. The fractional flow equation was developed from Darcy's law and deals with the location of the displacing front. Also, saturation and fractional flow of water at the front, the produced water oil ratio, saturation distribution and history behind the front as well as breakthrough times determine the performance of a waterflood.

The fractional flow equation is based on the general diffusivity equation, which can be expressed for a 1D case with constant density and incompressible flow as:

$$\frac{\delta q}{\delta x} + A\phi \frac{\delta S}{\delta t} = 0$$

Darcy's Equation for two phase flow:

$$q_o = -\frac{Kk_{ro}A}{\mu_o} \left(\frac{\delta P_o}{\delta x} + \rho_o g \sin \alpha \right)$$

$$q_w = -\frac{Kk_{rw}A}{\mu_w} \left(\frac{\delta P_w}{\delta x} + \rho_w g \sin \alpha \right)$$

Capillary Pressure: $P_{cow} = P_o - P_w$

Total flow rate: $q = q_w + q_o$

Fractional flow of water: $f_w = \frac{q_w}{q}$

Re-arranging the equations above leads to:

$$f_w = \frac{1 + \frac{Kk_{ro}A}{q\mu_o} \left(\frac{\delta P_{cow}}{\delta x} - \Delta \rho g \sin \alpha \right)}{1 + \frac{K_{ro}}{\mu_o} \frac{\mu_w}{K_{rw}}}$$

Capillary effects lead to dispersion and the resulting fractional flow curve will be higher.

Assuming negligible capillarity and gravity finally leads to:

$$f_w = \frac{1}{1 + \frac{K_{ro}}{\mu_o} \frac{\mu_w}{K_{rw}}}$$

This equation indicates that the water fractional flow is dependent on relative-permeability relationship (μ_o and μ_w are constant for a given reservoir pressure).

Buckley-Leverett Equation is used to calculate the waterflood performance. (Buckley & Leverett, 1942) The steps required for the calculation are drawing the fractional flow curve, drawing the tangent line, calculating oil recovery at breakthrough, calculating the time of breakthrough and finally calculating the oil production after breakthrough.

The frontal advanced theory for Buckley-Leverett Equation is based on the law of mass accumulation: *Input – Output = Accumulation*

$$[(q_w \rho_w)_x - (q_w \rho_w)_{x+\Delta x}] \Delta t = A \Delta x \phi [(S_w \rho_w)^{t+\Delta t} - (S_w \rho_w)^t]$$

For $\Delta x \rightarrow 0$ and $\Delta t \rightarrow 0$

$$-\frac{\delta}{\delta x} (q_w \rho_w) = A \phi \frac{\delta}{\delta t} (S_w \rho_w)$$

Using $\rho_w = \text{constant}$, $f_w = \frac{q_w}{q}$

$$-\frac{\delta f_w}{\delta x} = \frac{A \phi}{q} \frac{\delta S_w}{\delta t} \rightarrow -\frac{\delta f_w}{\delta S_w} \frac{\delta S_w}{\delta x} = \frac{A \phi}{q} \frac{\delta S_w}{\delta t} \rightarrow dS_w = \frac{\delta S_w}{\delta x} dx + \frac{\delta S_w}{\delta t} dt$$

If a constant saturation change during the displacement process is assumed, $dS_w=0$

$$0 = \frac{\delta S_w}{\delta x} dx + \frac{\delta S_w}{\delta t} dt \rightarrow \frac{dx}{dt} = \frac{q}{A\phi} \frac{\delta f_w}{\delta S_w} \rightarrow x_{S_w} = \frac{qt}{A\phi} \left(\frac{\delta f_w}{\delta S_w} \right)_{S_w}$$

Therefore, the advancing distance of the constant saturation front is directly proportional to time and the derivative at that saturation.

The position of the water front can be estimated as follows:

$$x_{wf} = \frac{W_i}{A\phi} \left(\frac{df_w}{dS_w} \right)_{S_{wf}}$$

$W_i = tq_t$ is the cumulative water injected at time t

To determine the velocity of the flood front, the fractional flow of water at the front and the water saturation of the front must be read out of the fractional flow diagram. Afterwards the following formula can be applied:

$$v_{wf} = \frac{q_t}{A\phi} \frac{f_{wf}}{S_{wf} - S_{iw}}$$

All saturations below S_{wf} travel at the flood front velocity.

To calculate the produced volume it has to be distinguished between the volume production before and after breakthrough.

Before breakthrough: $N_p = qt$

After breakthrough, where the saturation change is proportional to the produced volume, the following formula can be applied: $N_p = \frac{(\bar{S}_w - S_{iw})A\phi L}{B_o}$

Water-Oil-Ratio can be computed as follows:

$$F_{WO} = \frac{q_w}{q_o} \frac{B_o}{B_w} = \frac{f_w}{1 - f_w} \frac{B_o}{B_w}$$

2.4 Numerical Methods to Predict Waterflood Performance

The most important difference between the classical material balance approach and a reservoir simulator is that simulators take the locations of production and injection wells as well as their operating conditions into account. Numerical simulations are based upon material balance principles, taking reservoir heterogeneity and direction of fluid flow into account. Well rates and bottomhole pressures can be adjusted. Heterogeneity is honored by splitting the reservoir into small tanks, cells or blocks. For the simulation two phase flow equations (Conservation law), relative permeability data, capillary pressure data, the desired method of solution and PVT data is required. Nnaemeka Ezekwe (Nnaemeka, 2010) listed following important steps when setting up a numerical reservoir simulation model:

1. *Geologic Model Data*

Building a geologic frame work model of the reservoir that includes all faults and structural features that may affect fluid flow and identifying reservoir heterogeneities (permeability barriers, reservoir unconformities) is crucial to perform an appropriate characterization of the geologic model. Areal and vertical variations of reservoir properties like porosity, permeability, net sand thickness and saturations need to be captured.

2. *Fluid properties Data*

PVT properties of the fluids present in the reservoir are needed for the initialization of the model. For black-oil-simulators the PVT data is usually in tabular form. For compositional simulators the PVT data is an output generated with an equation of state.

3. *Rock/Fluid Properties Data*

Relative permeability and capillary pressure data as functions of fluid saturations are furthermore important input variables for the simulator. Also the compatibility of injection water and reservoir rocks should be analyzed to avoid undesired permeability reductions.

4. *Construct reservoir flow model*

Using the data from the previous steps the reservoir flow model is built. History-matching if prior production history is available is advantageous to increase the predictive capabilities of your reservoir model. Model equilibration data is used to define the initial state of the reservoir.

5. *Well Data*

Locations of wells, the grid system volume and type of produced and injected fluids are specified in this section. Furthermore time steps that define the speed and duration of the simulation are controlled by these data.

6. *Simulator Data Output*

A vast amount of data is generated as output. The optimum amount of data can mostly be selected by the user. At least well performance data and pressure and saturation distributions over time should be gained and visualized. Usually a base prediction case is performed with the current depletion strategy. Afterwards several predictive cases with different settings for injectors and producers can be performed and evaluated. This should finally lead to an optimized waterflood design with the best possible reservoir performance, considering economic considerations.

7. *Conduct a pilot waterflood project*

Especially for large waterflood projects it is recommended to have a pilot waterflood project to improve predictions before the waterflood design is implemented over the entire reservoir. This substantially helps in reducing uncertainties and risks.

2.5 Extension of Waterflooding

This chapter is only added for informative reasons as extended waterflooding techniques are not investigated closer in this thesis. It deals with the possible improvement of ordinary waterfloods by making use of tertiary recovery mechanisms that improve recovery by wettability alteration, interfacial tension reduction or mobility control.

One of the main forces opposing viscous flow are capillary forces, which are defined by the Laplace Young equation:

$$P_c = \frac{2 \sigma \cos\theta}{r}$$

Therefore the reduction of interfacial tension reduces capillary trapping and enables the oil droplets to flow more easily. The mobility mainly controls how easily fluids flow through porous media. Wettability describes the adherence of a fluid to a solid surface in presence of another immiscible fluid. Usually a water-wet behavior is favorable in terms of higher mobility of oil in the early stages and also in terms of wettability, as this would result in spontaneous imbibition of water into oil containing matrix. Oil will be driven out of the matrix and can be produced.

One of the fundamentals of EOR is the reduction of the capillary number. The capillary number is defined as:

$$N_c = \frac{u\mu}{\sigma \cos\theta}$$

As can be seen from the formula above the capillary number can be increased by increasing the fluid velocity u or the fluid viscosity μ or by reducing the interfacial tension σ . However

velocity (and also viscosity) changes that can be achieved are rather small compared to the reduction of interfacial tension which can be several orders of magnitude. Reducing interfacial tension is usually achieved by adding surfactants.

The capillary desaturation curve shows the relationship between residual oil saturation and the capillary number (See Figure 7). Different pore size distributions and the wettability of the system lead to different shapes of the capillary desaturation curve.

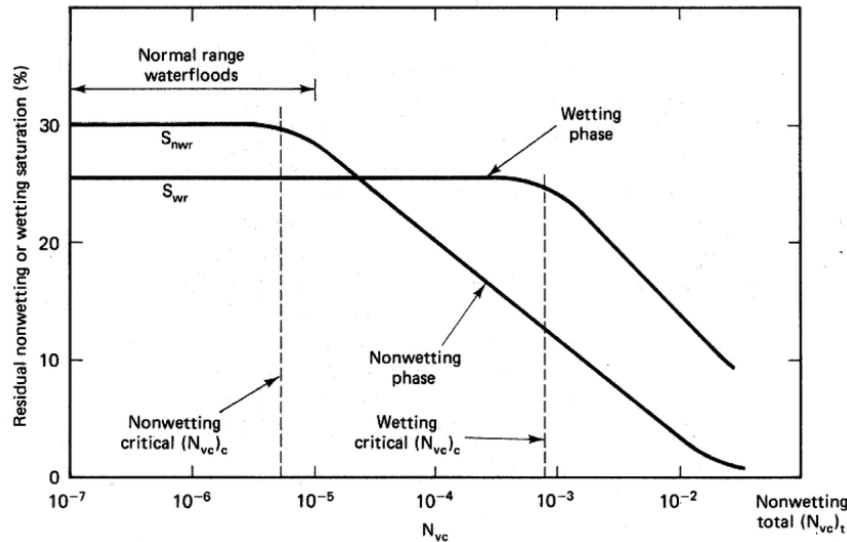


Figure 7: Schematic capillary desaturation curve (Kleppe & Skjæveland, 1992)

2.5.1 Smart Water Flooding

Smart waterflooding describes a waterflooding process where the ionic composition of injection water is modified. This leads to modified wetting properties of the reservoir to a more favorable state, so that the oil recovery could be improved. Smart waterflooding is also sometimes referred as low salinity waterflooding.

The main mechanisms besides the wettability alteration are dissolution and fine migration processes. Laboratory tests justified the advantageous effect of low salinity injection water. Oil recovery could be significantly increased for several experimental runs. Wettability alteration works in a way that acidic oil components are desorbed from rock surfaces which lead to more water wet rock surfaces. This is favorable, because the water breakthrough takes place at later times for water wet rocks compared to oil-wet rocks. Furthermore water imbibition is more likely, which provides additional driving force in terms of capillary forces that are added to the viscous forces. This might lead to the circumstance that more oil is driven out of the sample. It has to be outlined that some of these mechanisms are still under discussion and further research is necessary to understand the main mechanisms of low salinity waterflooding. (Mahani, et al., 2015)

A challenge for low salinity waterflooding is the sourcing and disposal of water. Seawater needs to be desalinated. This can be achieved either by thermal-based or membrane based methods. Thermal-based methods include distillation and mechanical vapor compression. Basically it can be described as heating saline water and condensing the vapor from the distillation process. Membrane-based methods are pressure driven. Pressure is applied to force the saline feed water through a membrane. Membrane-based methods are commonly favored since less space is required and also less energy is consumed during this process.

Low salinity waterflooding disturbs the initially established thermodynamic equilibrium in the petroleum system. To reach a new equilibrium (which is favored in terms of wettability alteration) a certain activation energy needs to be overcome. This means that temperature is a controlling factor in this process. For too low temperatures no reaction between oil components and mineral surfaces will take place. (Emad Walid Al Shalabi & Kamy Sepehrnoori, 2017)

2.5.2 Carbonate Water Injection

Another approach to increase the efficiency of waterfloods is to inject water saturated with CO₂. The CO₂ in the carbonated water diffuses into the oil without forming an individual CO₂ rich phase, which leads to oil swelling and viscosity reduction. The advantage of carbonated water over injecting CO₂ in a free phase is that the problem of gravity segregation is eliminated and furthermore sweep efficiency is enhanced due to a more favorable mobility ratio. Oil displacement and recovery is improved due to a higher viscosity and density of water, which affects the mobility ratio in a positive way. The mass transfer of CO₂ from water to oil is a result of the better solubility of CO₂ in oil compared to the solubility of CO₂ in water under same pressure and temperature conditions. Ultimate recovery of oil can be substantially improved by making use of oil swelling and a more favorable mobility ratio between water and oil.

The implementation of a carbonated waterflood is relatively easy as CO₂ can be simply separated from water and less gas has to be handled at the surface. Furthermore only limited modifications are required on the existing waterflood facilities. Nevertheless, some carbonate source is necessary which limits the locations where this technique can be applied. (Mehran, et al., 2011)

Chapter 3

Prediction of Performance: Analytical Analysis

The oil field of interest started production in 1966 and has an initial oil in place of 5.5 BSTB. The field was in natural depletion for 3.5 years. Until 2019 1.2 BSTB oil were produced, whereas around 1.4 BSTB water were injected since water injection started in 1970 to sweep the oil and maintain reservoir pressure. In total 137 producers, 40 injectors, 22 water source wells and 5 disposal wells are currently active.

PVT properties were provided from previous studies. Oil formation volume factor B_o , viscosity and solution gas ratio R_s are shown in Figure 8.

Bubble point pressure equals 2,530 psia. Water formation volume factor is 1.03 and water viscosity is 0.54 cp. Rock compressibility is $8.7E-06 \text{ psi}^{-1}$ and water compressibility is

$6.5E-06 \text{ psi}^{-1}$. Average initial water saturation in the carbonate unit is 20%. Gas-oil-ratio is around 500 scf/bbl.

The theoretically explained analytical concepts in chapter Analytical Methods to Predict Waterflood Performance are now applied to the field data. Furthermore material balance calculations are performed using MBAL. Results are shown below.

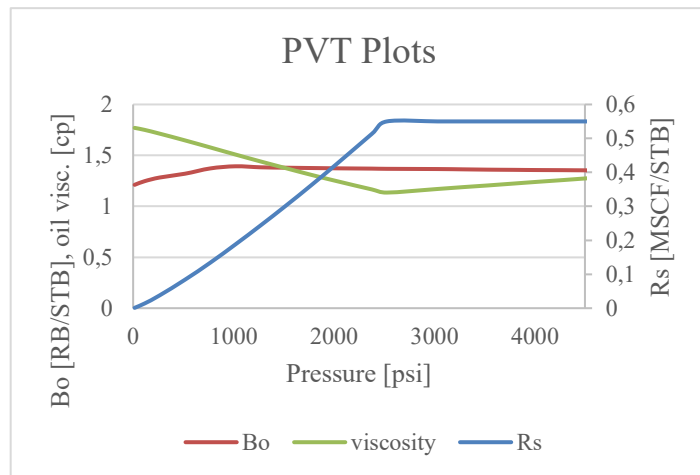


Figure 8: PVT properties

3.1 Pressure Analysis

Pressure data for static bottomhole pressure (SBHP) was provided by the operator at a datum depth of -8700 ft. A well by well quality check was performed to “clean” the data. Excessively high and most probably unrealistic pressure points were excluded. Especially data from injectors was investigated closely to exclude misleading high and low pressure values. The cleaned data set was then used for the further analytical analysis and as a simulation input.

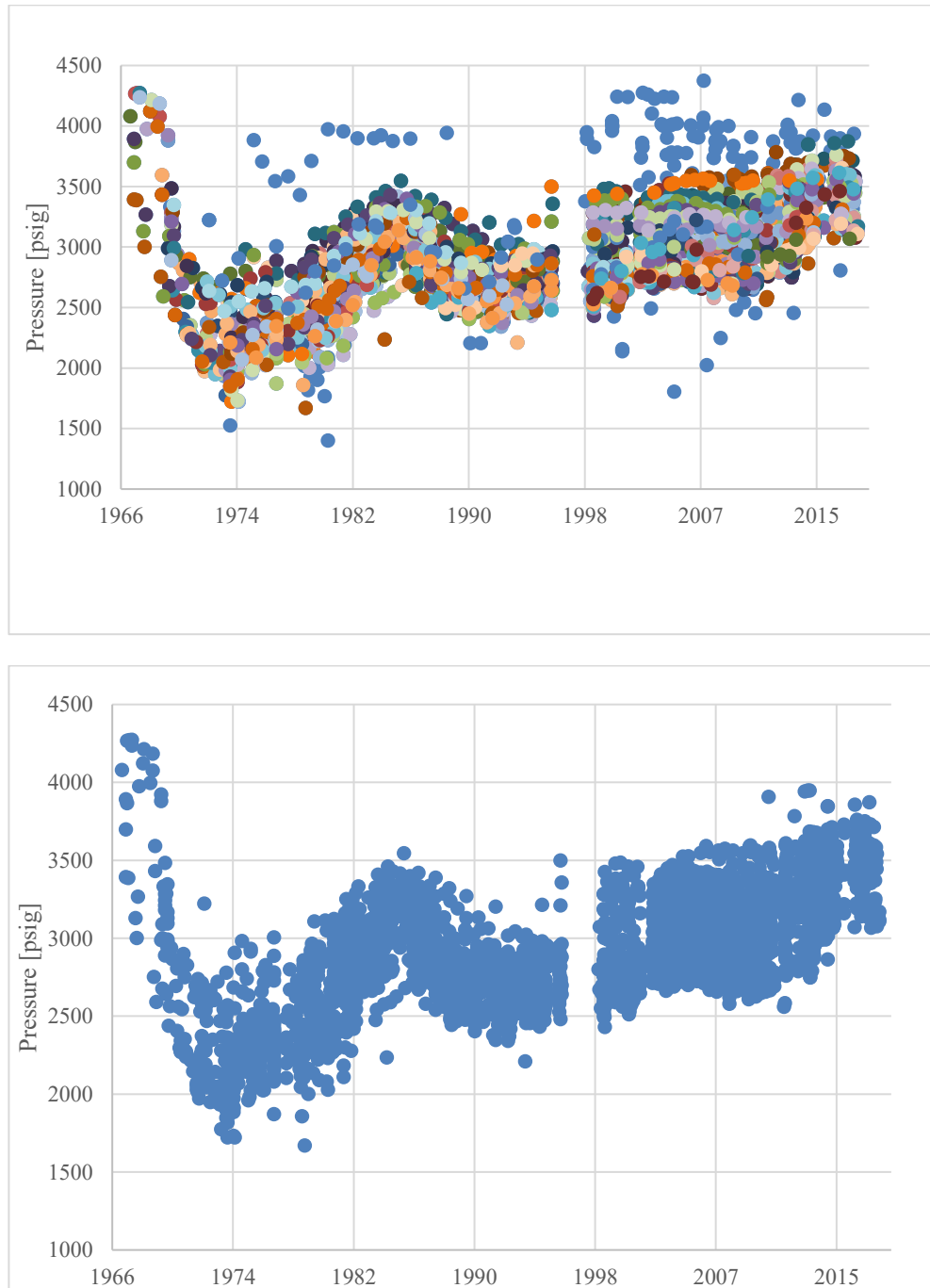


Figure 9: Pressure Analysis, raw and cleaned data

During further analysis of the pressure data with focus on the period between 1998 and 2013 three different pressure regions could be identified: low, increasing and high level. The increasing pressure region shows strongly increasing bottomhole pressures, whereas low and high level pressures remain approximately stable “at different levels” over the years. In Figure 10 the measured pressure values are outlined for the different regions. Pressure readings from the “high” pressure region are indicated in blue, those from the “low” pressure region are shown in green and pressure measurements from the “increasing” pressure region are shown in red.

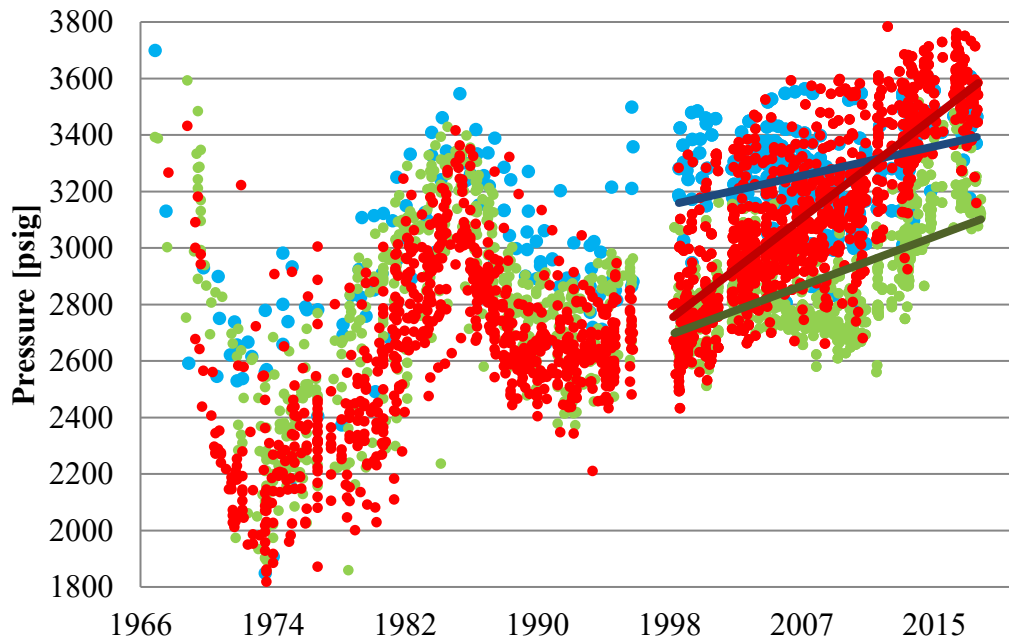


Figure 10: Different pressure regions (green=LOW; blue=HIGH; red=INCR)

The locations of the pressure regions outlined on the map are shown in Figure 11. Afterwards these pressure regions will be used in MBAL and Petrel to model the fundamental concept of geological features and dynamic data.

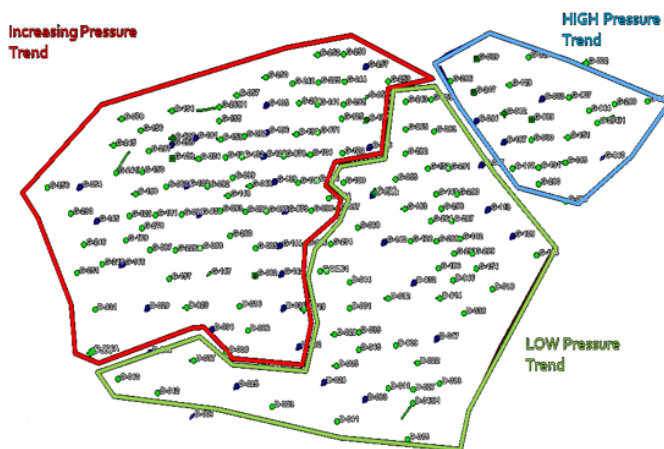


Figure 11: Pressure regions

3.2 WOR Analysis

Water/oil ratio is simply calculated by dividing water production rate by oil production rate. The WOR ranges from 0 (100% oil is produced) to infinite (100% water is produced). The WOR is closely linked to the ‘water cut’, which is the water production rate divided by the total production rate. If The WOR ratio equals 1, water cut results in 50%. (Bailey, et al., 2000)

To evaluate the efficiency of a waterflood system a semilog plog WOR vs. cumulative oil produced provides useful indications. As long as the water-oil ratio follows a linear trend, increasing the injection volume of water leads to an increased production. This plot gives useful indications if the field is producing acceptable water or if the water production is unacceptable and water control actions or water injection modifications should be considered.

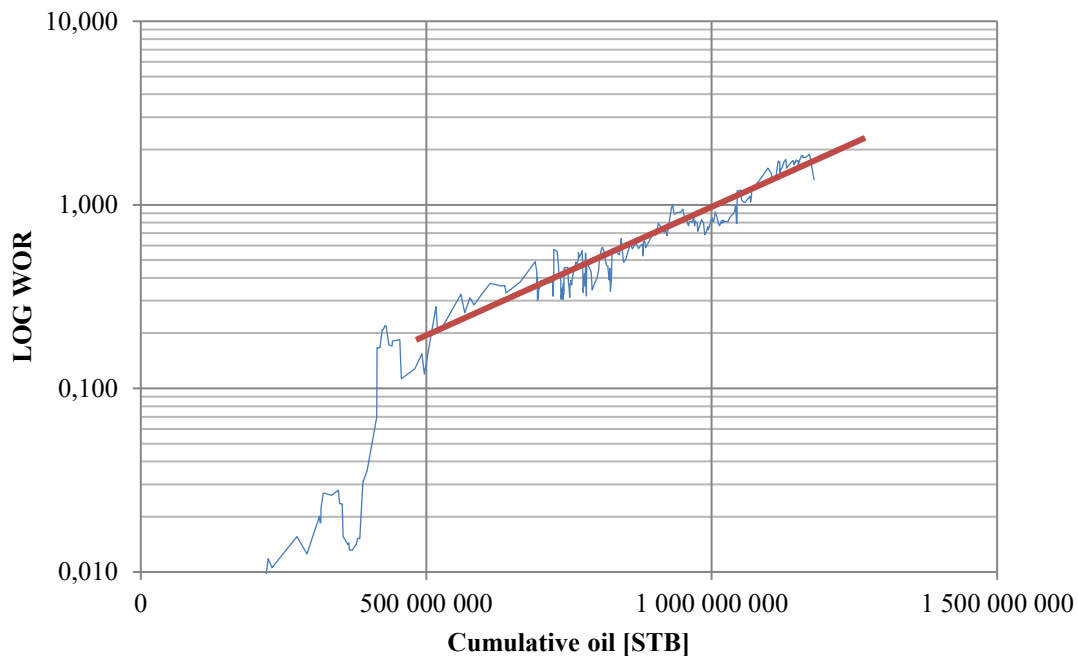


Figure 12: WOR whole field

The field has been subdivided into 12 blocks for analyses and simulation purposes. This concept was taken over from previous studies during the WOR-Analysis. The separation of the field into twelve sectors is outlined in Figure 13.

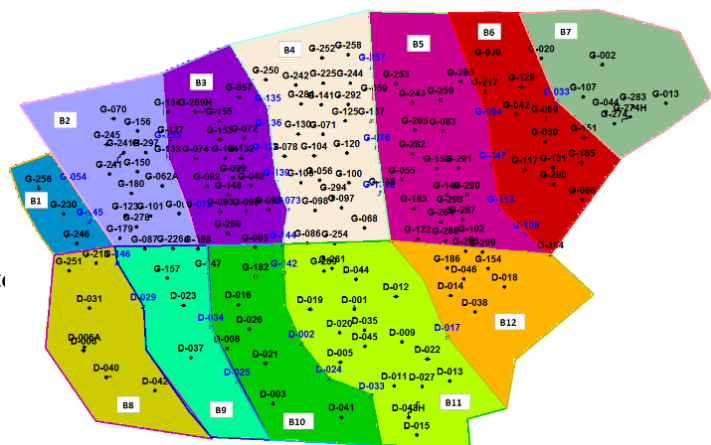


Figure 13: Division of the field into sectors

Looking at the individual sectors it was easy to identify high and low performing regions by their cumulative produced oil volumes. As clearly visible in Figure 14 the upper sectors are performing much better than the lower ones. Especially the sectors in the middle (3, 4, 5 and 11) show high cumulative oil production. This indicates that the line drive is efficient in this area. Sectors 1, 6, 7, 8 and 12 show a very poor behavior with high watercut and low cumulative oil volumes. These areas should be further considered for a change to a pattern flood instead of a line drive.

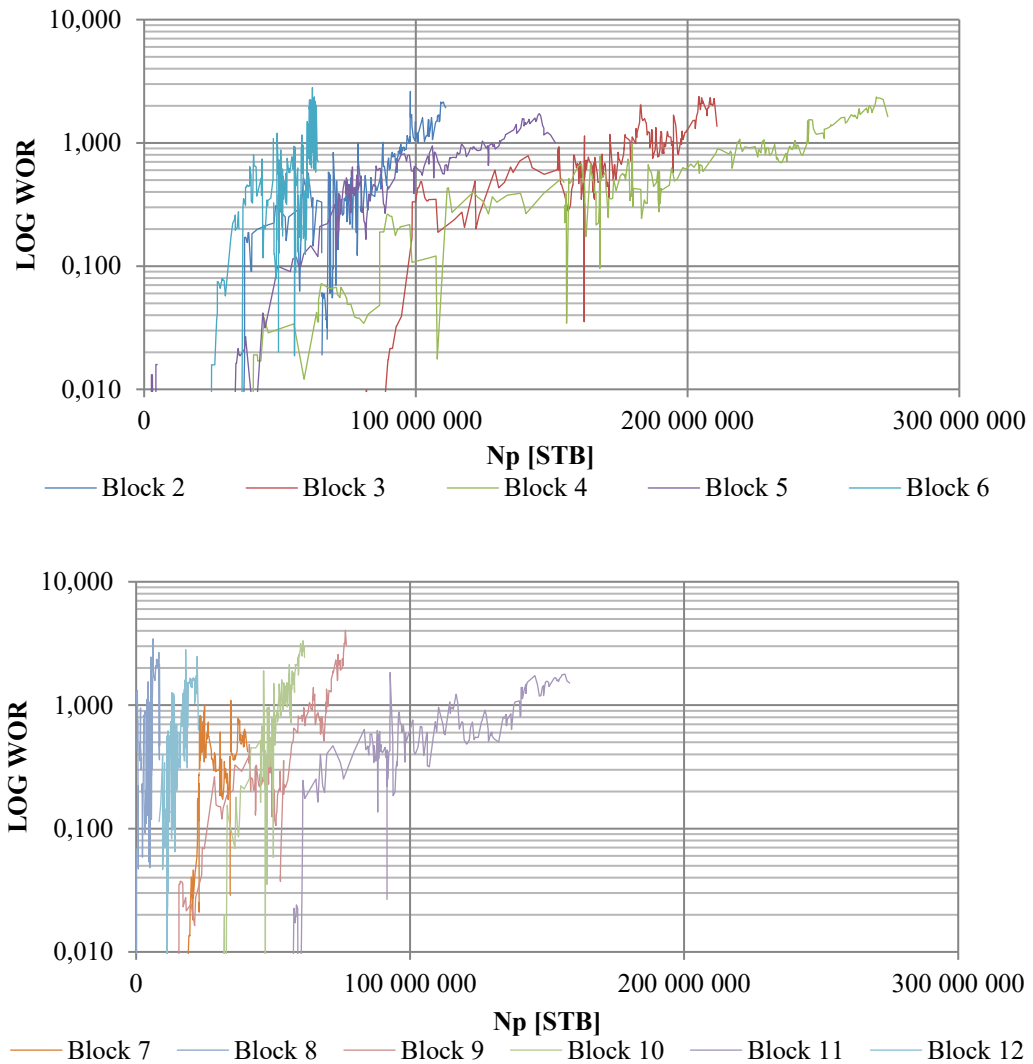


Figure 14: WOR of individual blocks

3.3 Water Cut Analysis

The current field water cut is at approximately 60%. Analysis of the water cut versus cumulative oil production on field level shows a quite stable linear trend as soon as injection of water started. The big potential that is still left and possible to produce is clearly visible on this simple plot. More than 350 MMSTB of oil are potentially left and able to produce by simply following the current production strategy.

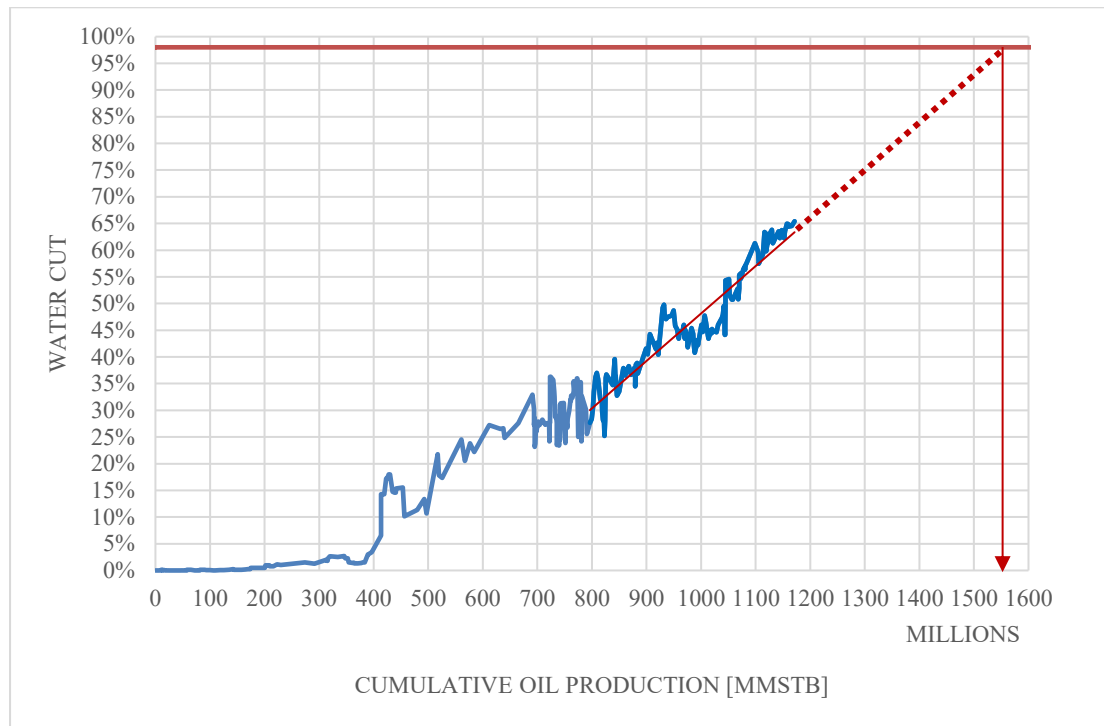


Figure 15: Water cut analysis

3.4 Determination of Volumetric Sweep Efficiency

To find out if there is additional oil recovery potential it is useful to determine the volumetric sweep efficiency of a waterflood. Cobb and Marek (1997) came up with an estimation procedure of the volumetric sweep efficiency if only historical oil production data is available. The method combines volumetric material balance concepts with basic waterflood principles. Parameters that must be known are cumulative oil produced from a waterflood since the start of initial injection N_p , oil formation volume factor B_o , floodable pore volume V_p , oil saturation S_o , connate water saturation S_{wc} and average water saturation in the water swept portion of the pore volume S_w .

Then the following formula can be applied to calculate volumetric sweep efficiency:

$$E_{vw} = \frac{\frac{N_p B_o}{V_p} + 1 - S_o - S_{wc}}{\bar{S}_w - S_{wc}}$$

The average water saturation in the water swept portion of the pore volume can be approximated from waterflood fractional flow theory.

Furthermore the formula can be re-arranged in a way that an equation of a straight line relating E_{vw} to N_p is obtained:

$$E_{vw} = A + BN_p$$

$$A = \frac{1 - S_{wc} - S_o}{\bar{S}_w - S_{wc}} = 0.7609$$

$$B = \frac{B_o}{V_p(\bar{S}_w - S_{wc})} = 2.18618E - 10$$

The connate water saturation is assumed to be 20%. The residual oil saturation at start of the waterflood is determined to be 45%. The average water saturation in the water swept portion of the pore volume was approximated to be 66% with waterflood fractional flow theory described by Craig (Craig, 1971). The oil formation volume factor is 1.39. From the start of waterflood in 1970 until 2018 0.9 MMSTB oil were produced. The floodable pore volume is 13.8E9 rbbl. Using this analytical approach from Cobb and Marek (1997) the vertical sweep efficiency is determined to be 0.761. It does not change significantly as more oil is produced (See Figure 16).

$$A = 0.7609$$

$$B = 2.18618E - 10$$

$$E_{vw} = 0.7611$$

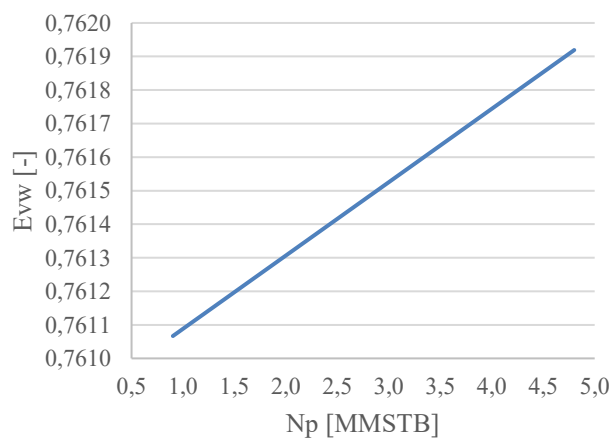


Figure 16: Analytically derived vertical sweep efficiency

3.5 Determination of Areal Sweep Efficiency

Areal sweep efficiency can be estimated by Fassih representation of Dyes et al Model. This correlation is applicable at and after breakthrough for 5-spot, direct and staggered line drive. The following formulas were applied:

$$E_A = \frac{1}{1 + A}$$

$$A = [a_1 \ln(M + a_2) + a_3]f_w + a_4 \ln(M + a_5) + a_6$$

Most recent data shows a water-oil-ratio of 1.371 which results in a fractional flow of water of 0.578 and a mobility ratio of 0.73. Using literature values for the coefficients a1, a2, a3, a4, a5 and a6 the areal sweep efficiency for a direct line drive was determined to be 0.79. The areal sweep efficiency for the staggered line drive is 0.86 and for the 5-spot-Pattern it is 0.87.

3.6 Buckley Leverett Frontal Advance Theory

Two approaches for the analytical estimation of the waterflood performance utilizing Buckley Leverett Frontal Advance Theory were applied. One was to analyze the behavior of a complete injection line and the other was to take a closer look at one specific representative injector.

An injection line from the middle region (indicated in pink color in Figure 17) was selected. The flood area was estimated by the length of the injection line (12 km) and the average height of each layer (F 97 ft, G 51 ft and H 60 ft). A net to gross ratio of 0.5 was applied.

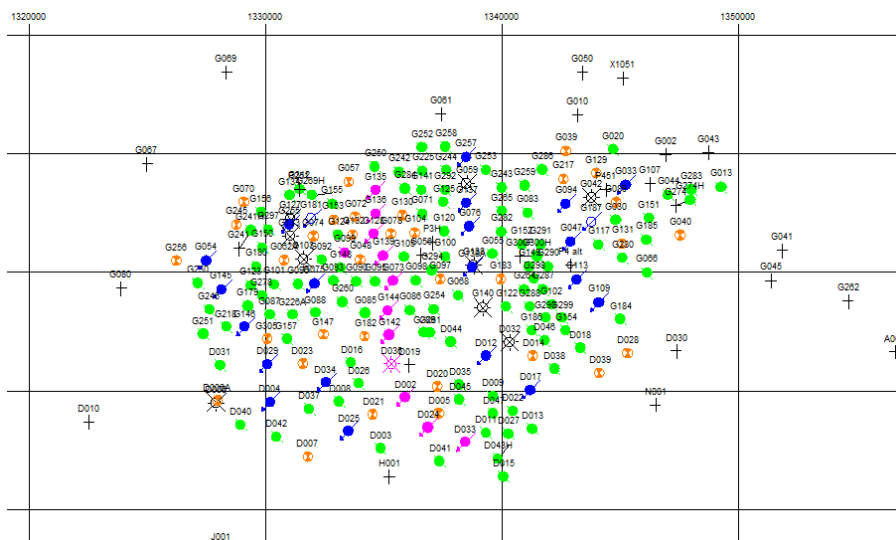


Figure 17: Injection line for BL analysis

Porosity values for each layer were provided (F 15.3%, G 14.1%, H 14.5%). The average injection rate was calculated from historical injection volumes. For simplicity it was assumed,

that the injected volume spreads equally in both directions. This results in a total average injection rate of 17,500 STB/day. Relative permeabilities were calculated using Brooks Corey relative permeability model. End-point relative permeabilities were given from former analysis. The irreducible water saturation is determined to be 30%. Residual oil saturation is 18.6%. Oil viscosity is 1.13 mPas and water viscosity is 0.54 mPas. The resulting relative permeabilities for the three main reservoir layers F, G and H are shown in Figure 18.

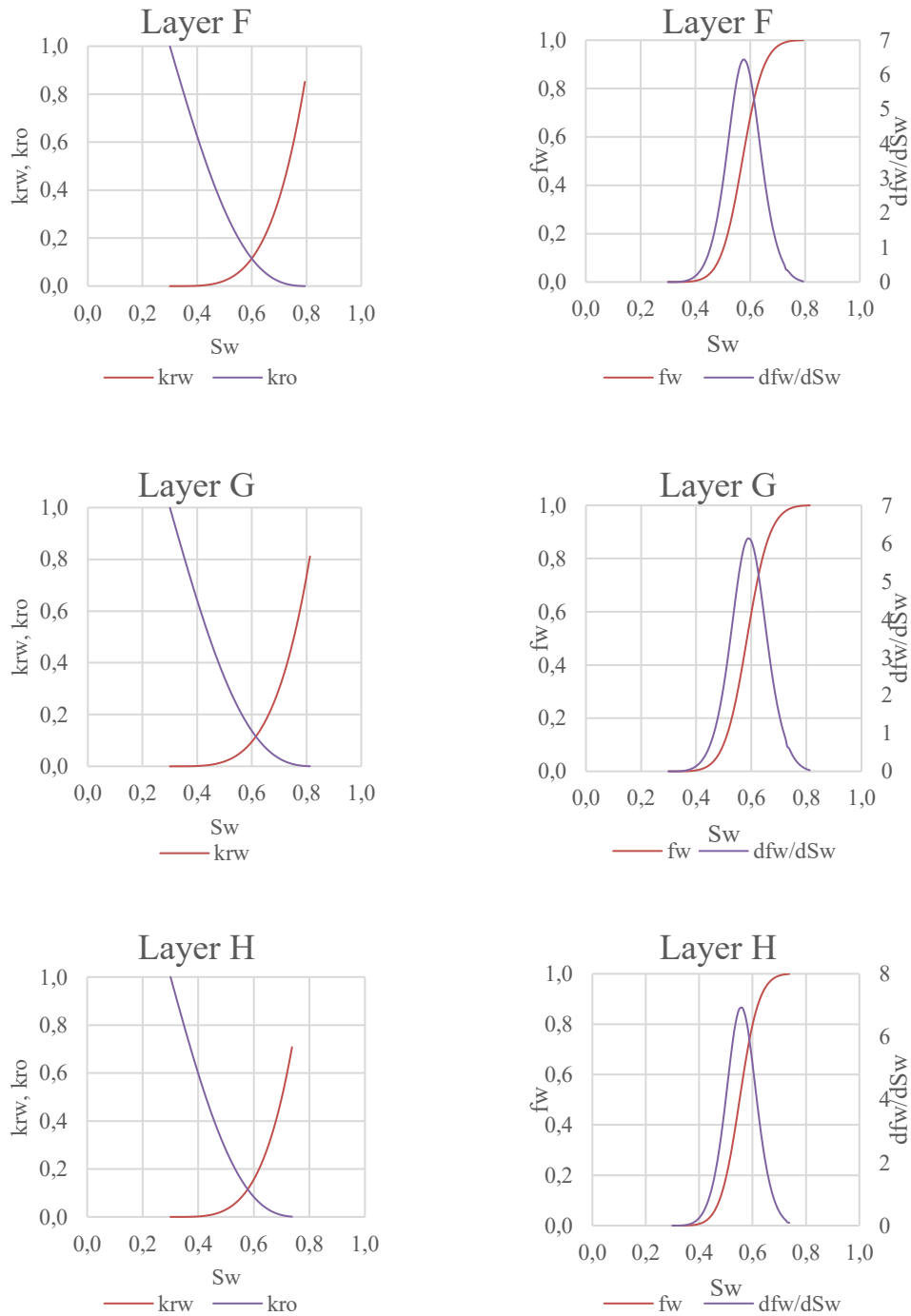


Figure 18: Rel. permeabilities and fractional flow curves layers F, G and H

The resulting Buckley Leverett profile is shown in Figure 19. The water front moved between 1,300 and 2,000 ft in the individual layers within 3 years of injection.



Figure 19: BL profile for injection line

Furthermore the calculation was performed for one specific injector (G-073). Injection rate was again estimated from historical injection rates and resulted to be around 4,500 STB/day. Again the rate was simply divided by 2 under the assumption of an equal distribution in both directions. The flood area equals half of the distance to the next injector multiplied again with the average height of the individual layer (F, G and H) and the net to gross ratio. The propagation of the front for this injector is between 2,100 and 2,600 ft for 3 years of injection.

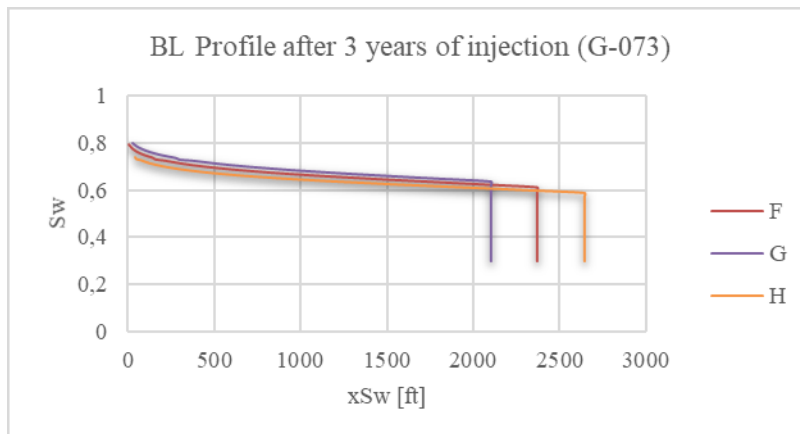


Figure 20: BL profile for G-073

3.7 Material Balance Calculation

Another analytical approach to analyze the reservoir was to create simple tank models using MBAL. Utilizing material balance equations, main drive mechanisms should be evaluated to better predict future production and understand historical behavior. Cumulative oil and water production, cumulative water injection and pressure data was considered on field basis (see Figure 21) as well as for the three pressure regions determined during pressure analysis. (See Figure 22). Values of the "Low" pressure region are outlined in green, values of "High" pressure region are shown in blue and "Increasing" pressure region values are red.

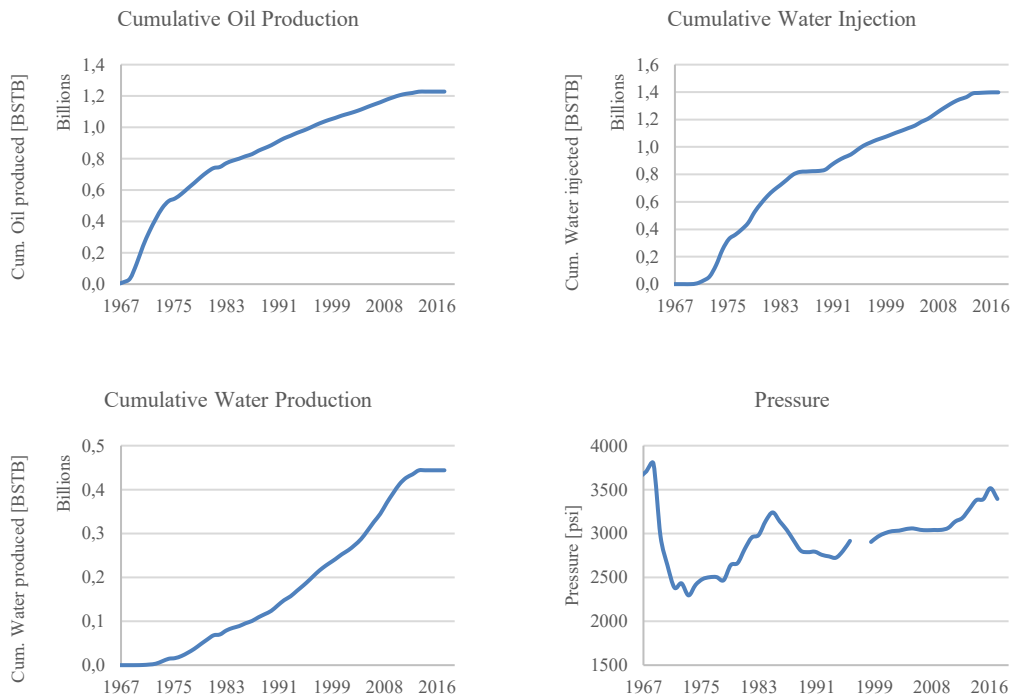


Figure 21: Oil production, water production & injection, pressure on field basis

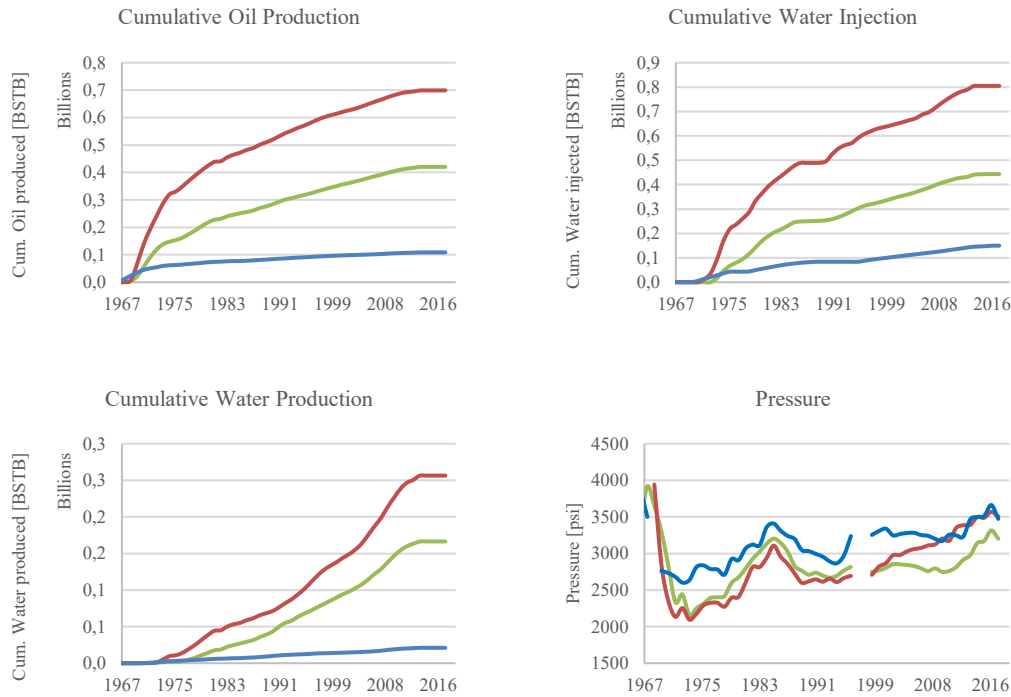


Figure 22: Oil production, water production & injection, pressure for pressure regions

3.7.1 Single Tank - Full Field

Looking at the unmodified data as shown in Figure 23 it is visible that during early times the simulation follows the actual pressure trend. Nevertheless the simulated tank pressure is constantly too high from 1971 until 2003, where it drops below the measured values. For this run an original oil in place of 5.5 BSTB was used (as reported from former field studies).

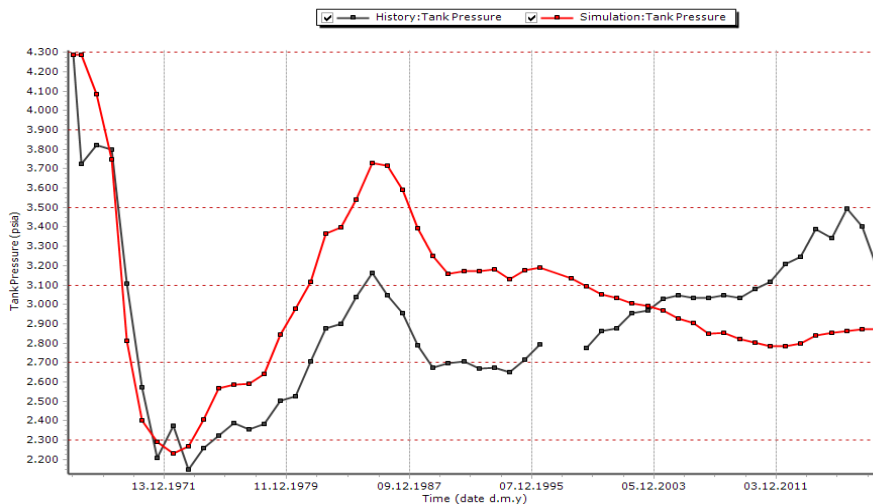


Figure 23: MBAL – full field simulation, original

One possibility to better match the pressure is to adjust the injected water volume. Possible explanations for incorrect injection volumes that does not support the pressure of the field could

be errors in the reported injection volumes, losses due to casing leaks or extensive injection into the granite basement. It turned out that injection volumes are lost in the first period of production and some additional influx from 2000 onwards is required to match the profile. A reasonable match could be achieved as shown in Figure 24.

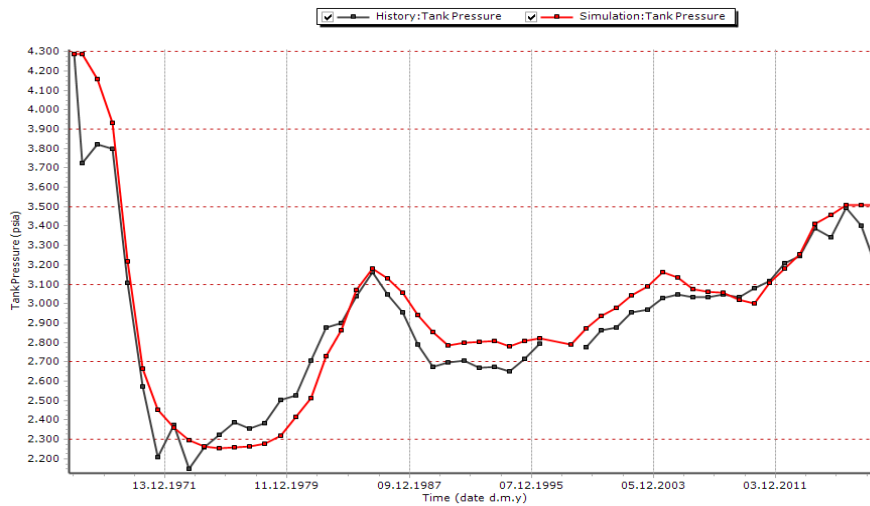


Figure 24: MBAL – full field simulation, adjusted injection rates

Another approach was to decrease the original oil in place by regression. It turned out that an original oil in place volume of 4.35 BSTB leads to a much better match. To further improve the match the porosity was decreased. This could be an indication that the estimated porosity of 12% is maybe too high.

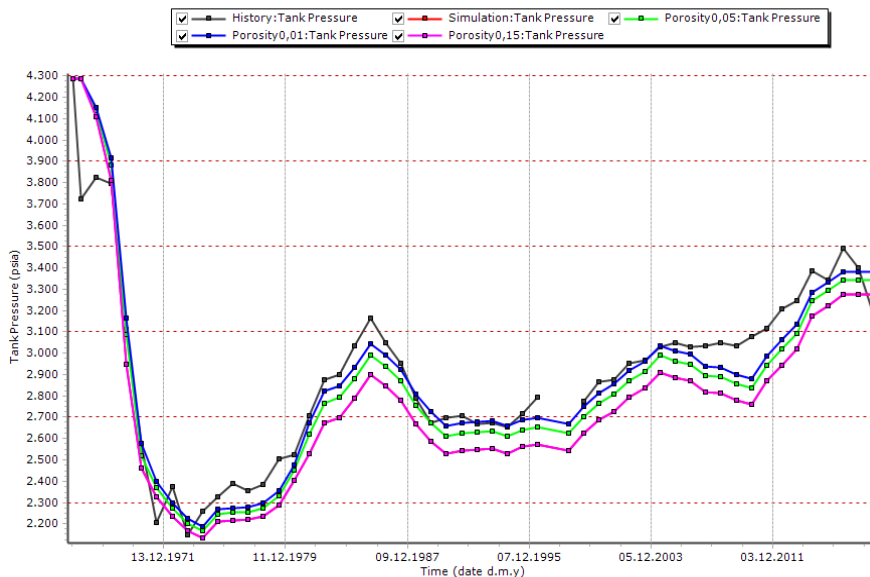


Figure 25: MBAL – full field simulation, adjusted OOIP

3.7.2 Multi Tank - Pressure Regions

To increase the significance of the simulation, a multi-tank MBAL model, as shown in Figure 26 with three interacting tanks for the low, high and increasing pressure region was created.

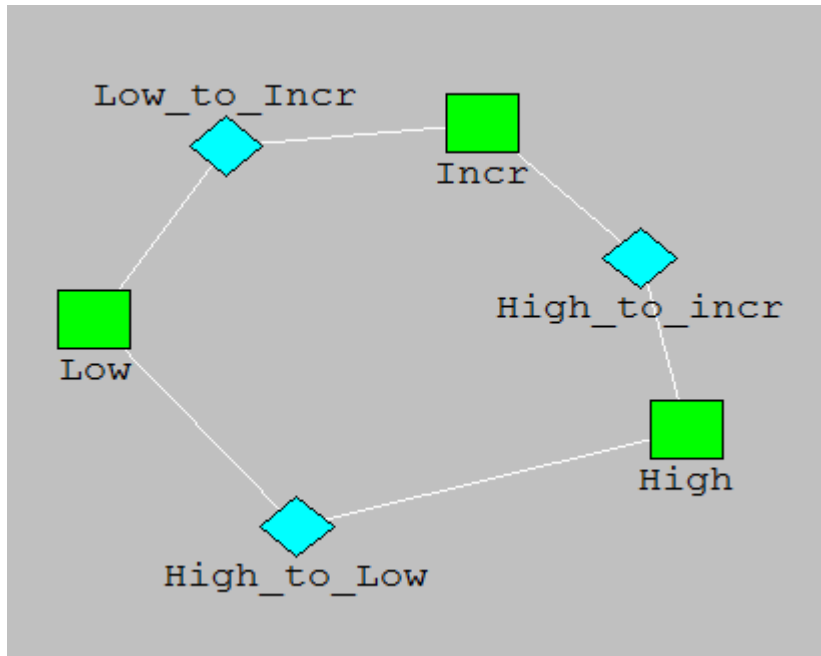


Figure 26: MBAL model - multitank

Transmissibilities between these tanks were defined by regression. Again the original simulation profile for the tank pressure was most of the time much too high in comparison to measured values (See Figure 27).

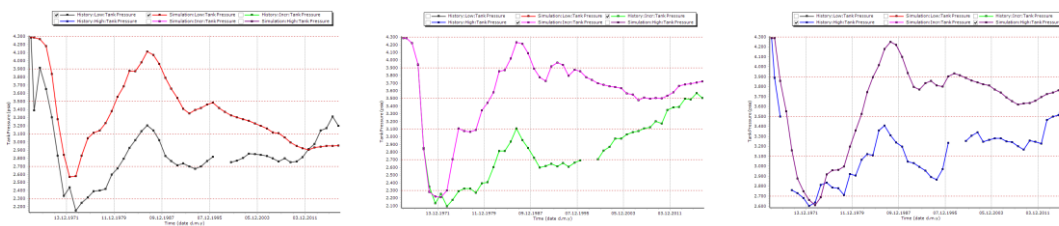


Figure 27: MBAL – pressure regions, original data

To decrease the simulated pressure, injection volumes were decreased for the first period (1974-1981). Possible explanations for the lost injection water are errors in the reported injection volumes, casing leaks or extensive losses to the granite basement, as mentioned earlier. From 1997 on additional influx (to the injected water) is necessary to match the historical pressure values. Transmissibilities were again determined by regression. Finally the following profiles were computed:

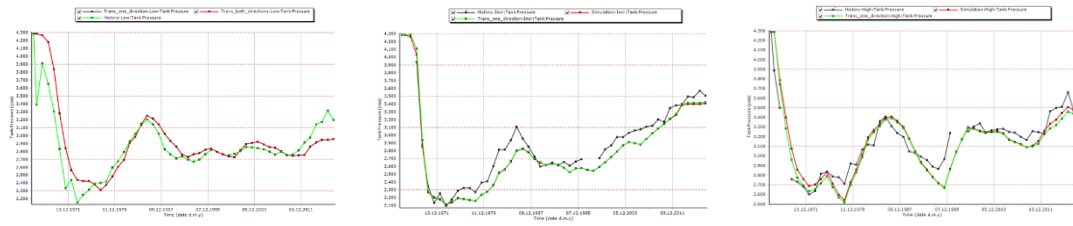


Figure 28: MBAL – pressure regions, adjusted injection rates

After adjusting the injection rates for the full field averaged data as well as for the individual pressure regions the applied modifications revealed a common pattern: Fluid losses shortly after water injection started in 1970 and additional influx from 1998 onwards (See Figure 29). One explanation would be that an aquifer influences the pressure behavior and delivers additional water to increase the reservoir pressure. Nevertheless, it also has to be kept in mind that errors in the reported injection volumes are possible.

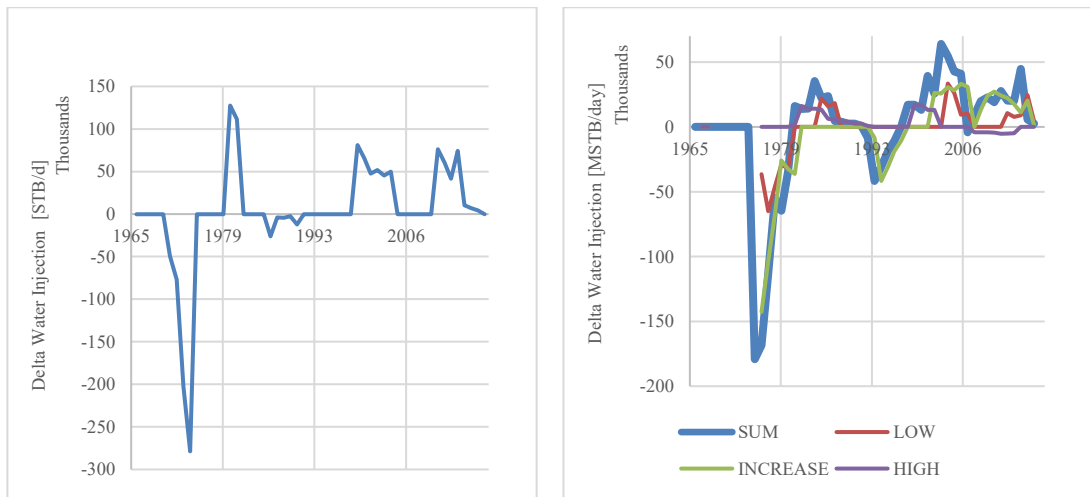


Figure 29: Comparison of water injection modifications

3.7.3 Multi Tank - Pressure Regions with Loss Zones and Aquifer

Fluid losses and possibly an aquifer influence the pressure behavior and extract or deliver water to decrease or increase the reservoir pressure. Based on these findings another MBAL model was set up. (Figure 30)

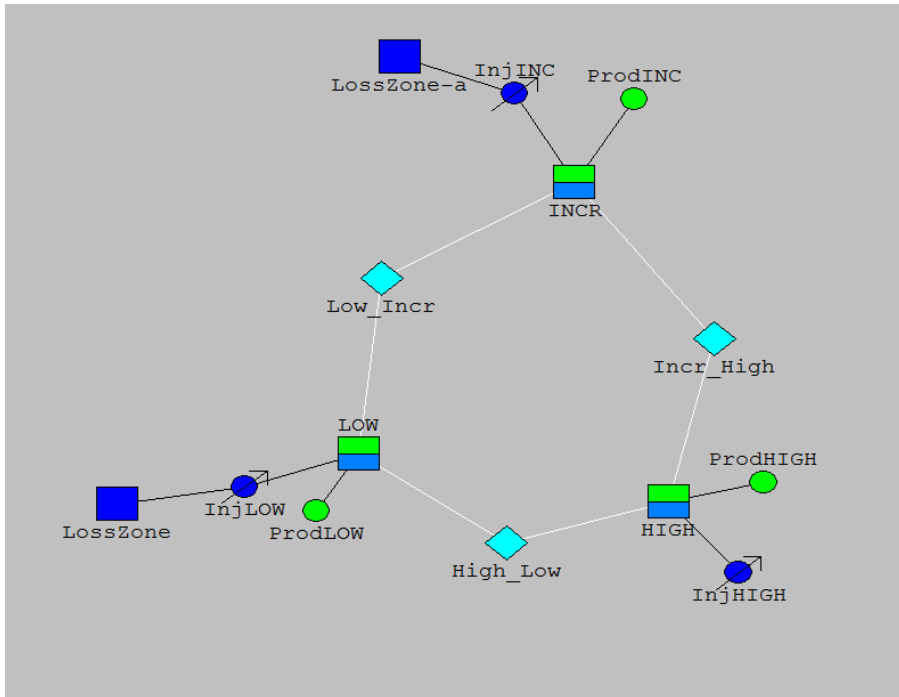


Figure 30: MBAL model - multitank extended

Two additional tanks represent loss zones for the “low” and “increasing” tanks. Injection volumes were allocated based on the former determined lost injection volumes. Aquifer support was introduced with the “Van Everdingen Hurst” analytical aquifer. Aquifer parameters were guessed and afterwards a regression was applied. Finally a reasonable history match was achieved that represents the pressure behavior in the different areas:



Figure 31: MBAL – pressure regions, loss zones and aquifer

An OOIP of 4.4 BSTB led to the best match. Pressure was generally too high for an OOIP of 5.5 BSTB. This indicates once again, that the estimated oil in place of 5.5 BSTB could be too optimistic. Figure 32 shows the cumulative aquifer influx in the low, increasing and high pressure zone. Especially for the increasing region the aquifer influx is very high and therefore influences the pressure profile substantially.

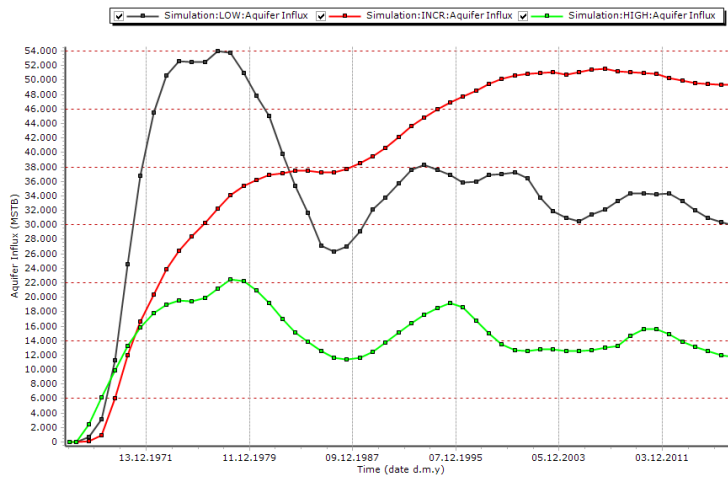


Figure 32: MBAL – pressure regions, aquifer influx

Cumulative oil production is matched in all cases as shown in Figure 33.

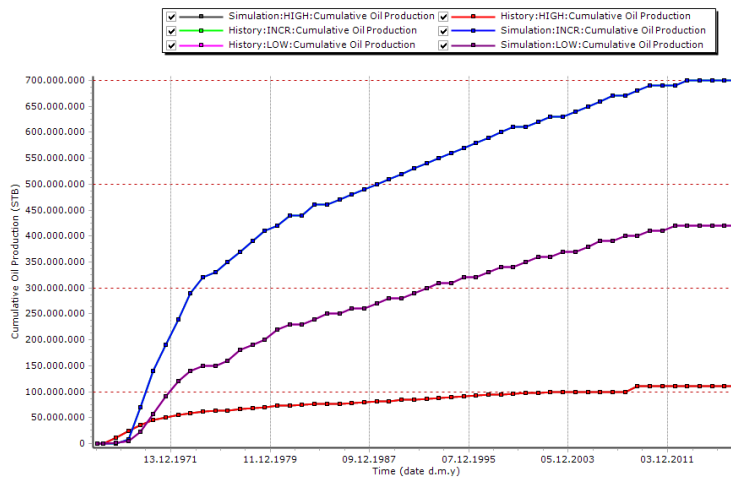


Figure 33: MBAL – pressure regions, cumulative oil production

Chapter 4

Prediction of Performance: Numerical Analysis

To transfer analytically derived results into a numerical reservoir model, simple block models with average reservoir properties were created using Petrel and simulations were performed using Eclipse Black Oil simulator. Afterwards findings from this block modelling process are applied to field scale to determine infill well locations and an improved producer/injector setting.

For the simple block models no structural features were considered. Homogeneous blocks with different layer properties were created. Layer properties porosity, permeability and initial water saturation were averaged from the full field model. Average properties were used to better compare numerical results to analytical results. The blocks are slightly different in size, but have an approximate extension of 2 x 2 km. The following patterns were taken into account (See Figure 34):

- Base case (current well setting)
- 5 spot pattern with large spacing (approx. 1.5 km) normal and inverted
- 5 spot pattern with small spacing (approx. 0.75 km) normal and inverted
- Line drive large spacing (approx. 1.5 km)
- Line drive small spacing (approx. 0.75 km)

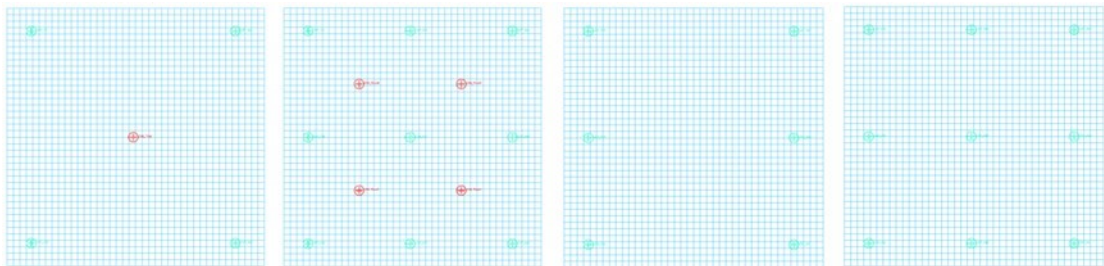


Figure 34: Well settings 5 spot large/small spacing, line drive large/small spacing

Three blocks were built in the low, increasing and high pressure region. (See Figure 35) These blocks were chosen such that each of them represents one region of the beforehand identified pressure regions with “Low”, “High” and “Increasing” pressure trend. The blocks have no-flow boundaries and were treated as closed tanks. This simplification is only applied for the homogeneous block modelling as a “first-look” interpretation. For the simulation of the whole pressure sector (See chapter 4.4), effects of the surrounding formation are taken into account.

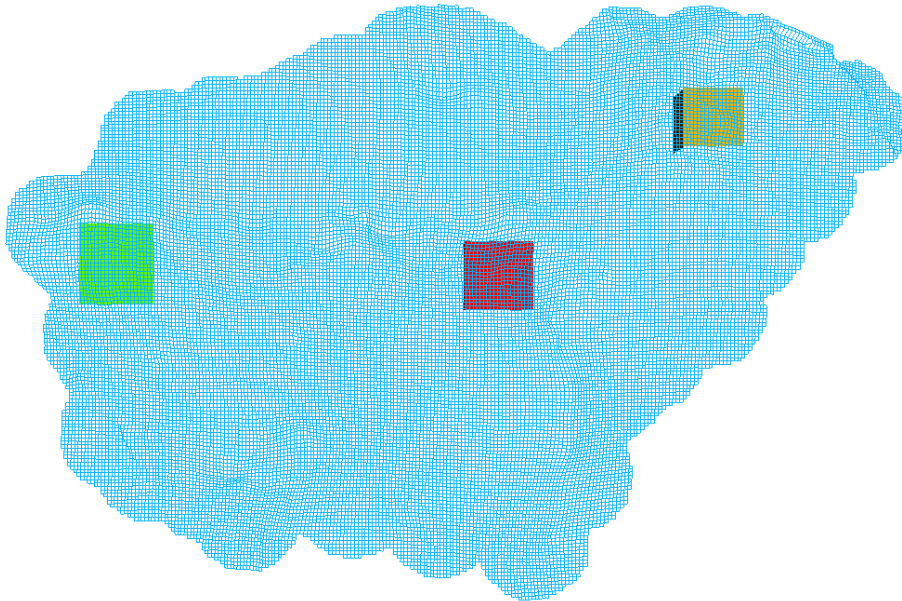


Figure 35: Location of blocks (green=increasing; yellow=high; red=low)

Actual field data was approached between 1966 and 2019 with a maximum deviation of +/- 15% to the real data. To make sure that the simulation results of the homogeneous blocks are representative, the same development strategy was applied to an exported sector of the corresponding area in the field. The homogeneous block and the exported sector of the LOW pressure region are shown in Figure 36.

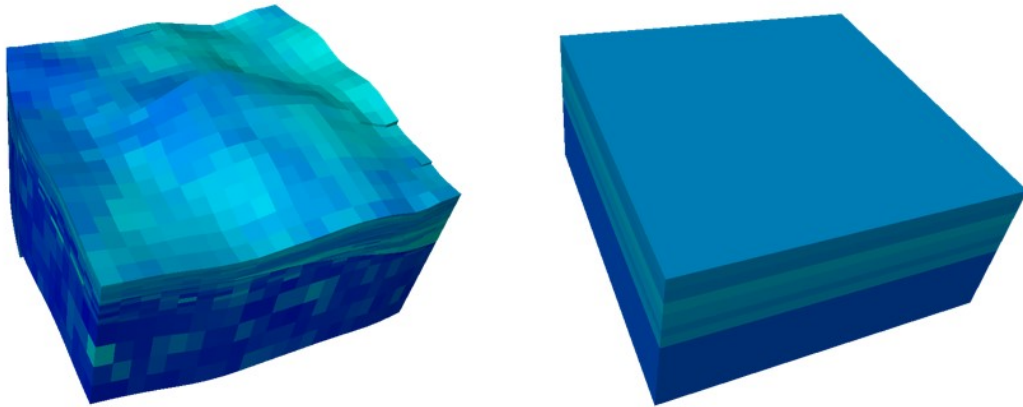


Figure 36: Block LOW; exported block and homogeneous sector model (porosity)

As an example, the resulting recovery factor against the field water cut was calculated and plotted for both models (homogeneous block and exported sector). The resulting profile is shown in Figure 37. Although no structural features are considered in the homogeneous block, there is not a huge difference in oil recovery to the exported sector, which considers those structural features as well as a property distribution. Overall the simulated recovery is around 10% too high for the homogeneous block. This circumstance should be kept in mind later on.

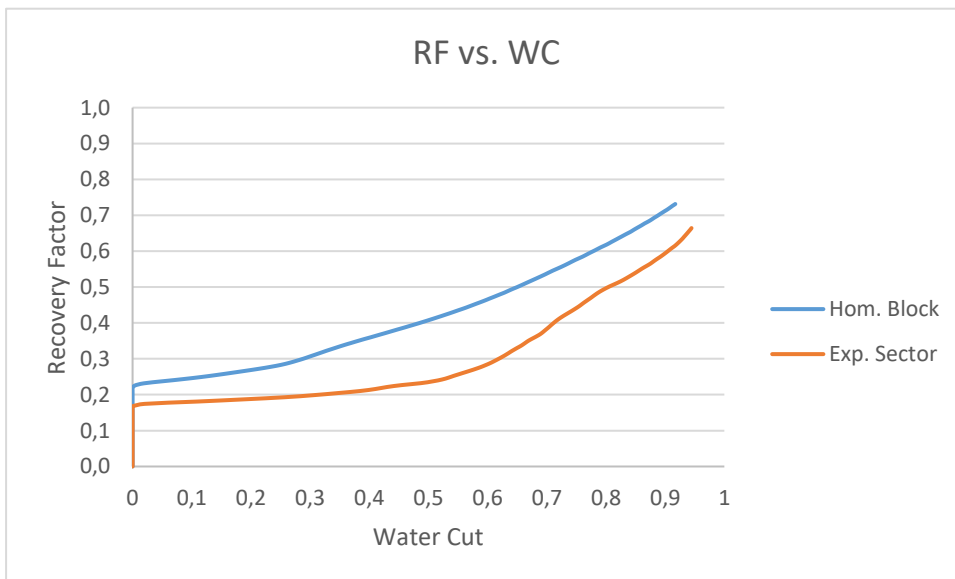


Figure 37: Block LOW; comparison homogeneous block to exported sector

Historical injection rates were averaged according to the documented injection rates of the injectors in each specific area.

After 2019 the production/injection pattern was modified to reveal the beneficial effect on the recovery efficiency in case of different well settings. To compare the result, also the current injection strategy was simulated. This setting is called “base case”.

The injection rate for each injector well was chosen to be 4,500 STB/day according to historical injection rates. Simulation was stopped either if a water cut of 98% was reached or after 180 years of simulation. To make the results better comparable, dimensionless numbers (pore volume injected and recovery factor) were used for the analysis. Those numbers were calculated as follows:

$$\text{Pore volume injected (PV inj)} = \frac{\text{cumulative water injected}}{\text{pore volume}}$$

$$\text{Recovery factor (RF)} = \frac{\text{cumulative oil produced}}{\text{Oil initially in place}}$$

4.1 Block: Low

Porosity, permeability and initial water saturation were averaged layer-wise from the full-field reservoir model provided by OMV. Figure 38 visualizes the 3D properties of the exported sector of the full-field-reservoir model (left) next to the properties of the homogeneous block model.

The historical production performance of this region is better than for the other two blocks. After 47 years of injection (starting from 1972 until 2019) the current water cut is at about 50%. In this region there are currently two injectors and three producers active. (See Figure 39)

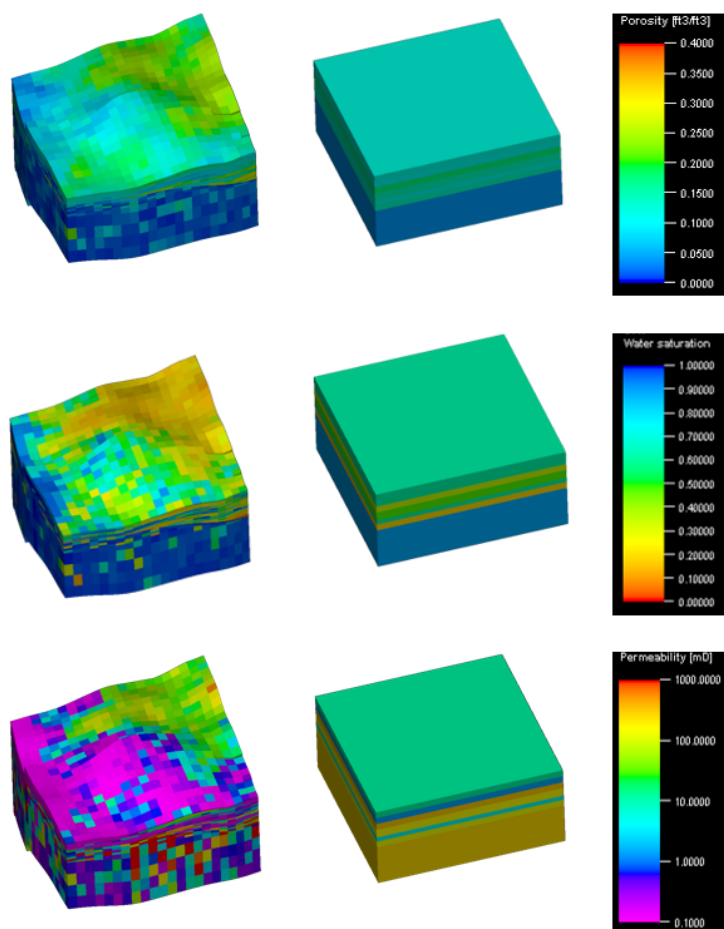


Figure 38: Block LOW; porosity (top), initial water saturation (middle) and permeability (bottom), exported sector and homogeneous block

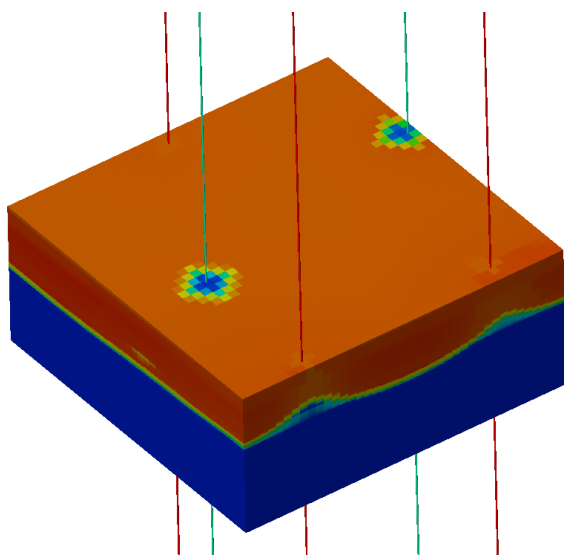


Figure 39: Block LOW; simulated oil saturation in 2019

The distance between two injectors is approximately 3 km in this part of the field. By leaving the injection pattern unchanged the ultimate recovery factor would be 61.1%. Modifying the injection pattern would increase the ultimate oil recovery only by 0.7% in the very best case, which is a 5 spot pattern (inverted) with an injector-injector distance

of 800m. Comparing the additional recovery for one pore volume injected shows that the cumulative oil production could only be enhanced by 1%. The oil saturation of the block after the injection of one pore volume for the current well setting and a modified 5-spot-pattern is shown in Figure 40. This minor improvement of recovery efficiency clearly indicates that modifying the injection pattern in this section of the field is not economic and therefore not recommended.

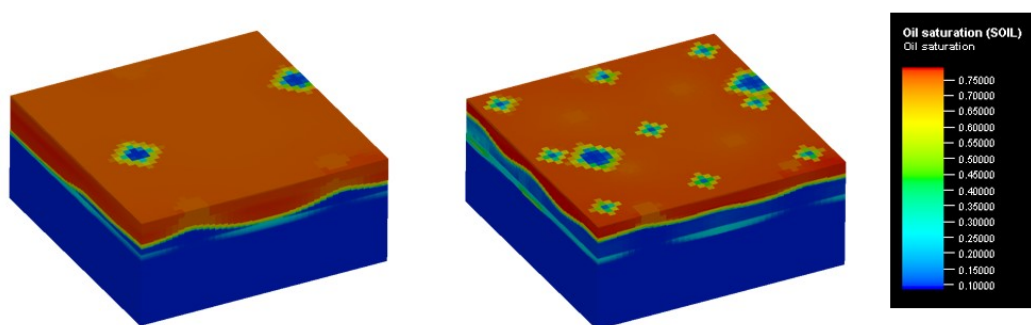


Figure 40: Block LOW; oil saturation 1 PV injected, base case vs 5 spot pattern

In Figure 41 recovery factors for all simulated injection patterns are visualized. The base case in red has the second highest recovery efficiency. This again shows that there is no need to modify the injection pattern in this area.

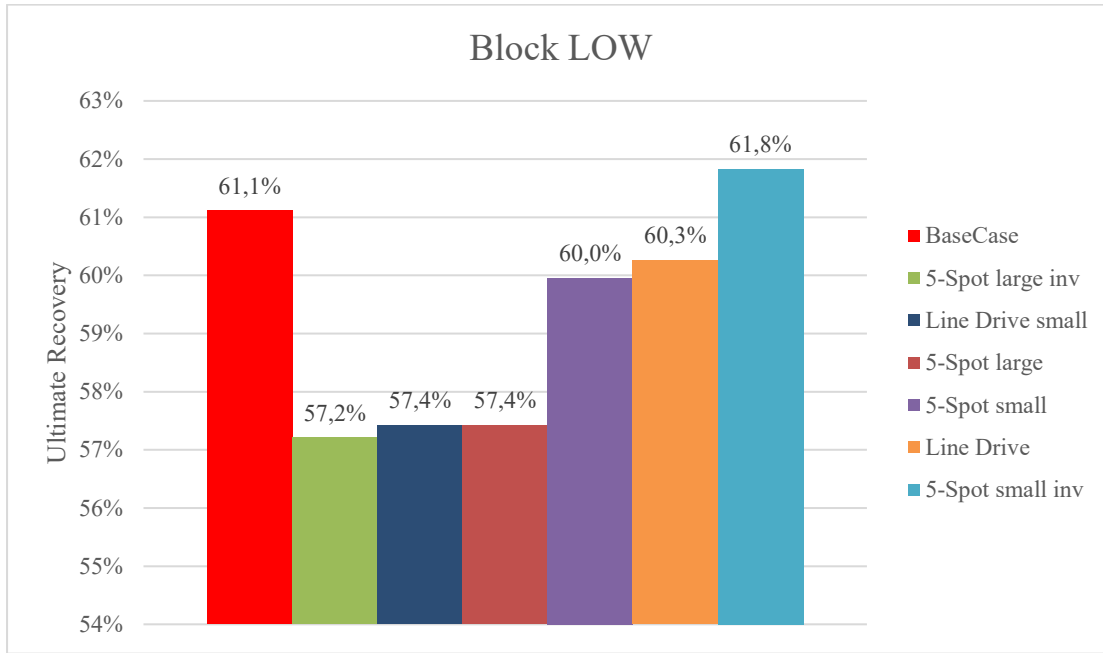


Figure 41: Block LOW; Ultimate Recovery for different Patterns

4.2 Block: High

Again, the 3D properties porosity, permeability and initial water saturation were averaged layer-wise from the full-field reservoir model provided by OMV. In Figure 42 3D properties of the exported sector of the full-field-reservoir model (left) next to the properties of the homogeneous block model are shown.

The historical production performance of this section is rather poor according to the WOR-Analysis. Water injection started in 1969. The original injector spacing is approximately 2.7 km. Only very few injector wells are currently active in the whole “High” region. In the selected

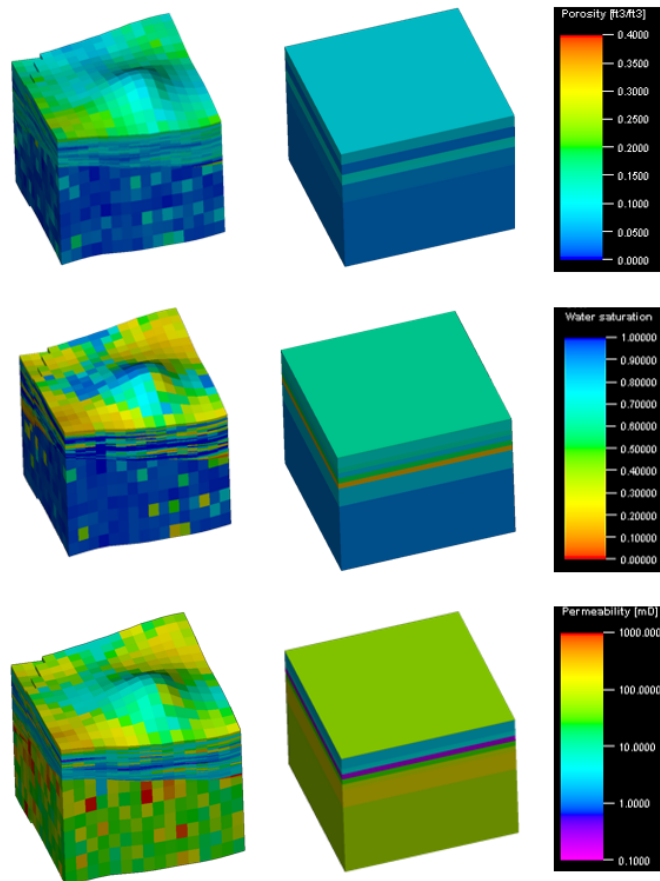


Figure 42: Block HIGH; porosity (top), initial water saturation (middle) and permeability (bottom), exported sector and homogeneous block

block there is one injector well and three producer wells active (at the moment). (See Figure 43) Current reported field water cut is at 40% in this region.

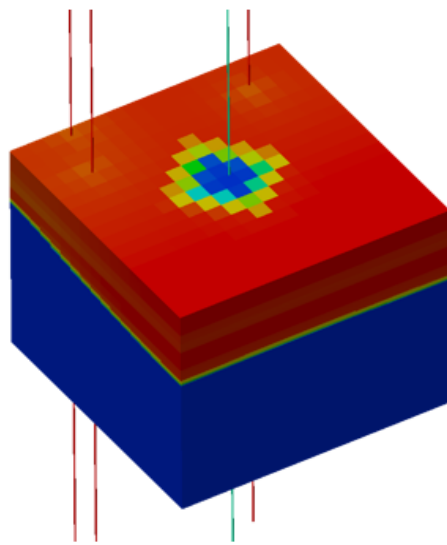


Figure 43: Block HIGH; simulated oil saturation in 2019

The simulated recovery factor until 2019 is 32% for a production period of 50 years. The ultimate recovery factor for the current well setting would be 49%. Changing the pattern to increase the areal sweep efficiency would increase the recovery factor to 63% in the best case, using a 5-spot-Pattern inverted with reduced spacing of 750m. The recovery factor after injecting water at a rate of 4,500 STB/day per well for 20 years was compared. In this case the recovery could be improved from 37%

to 47% for a 5-spot-Pattern flood. This indicates that drilling additional wells in this section could improve the recovery significantly and is very likely economic.

Figure 44 shows the oil saturation of the different patterns in 2039. This visualization clearly indicates the beneficial sweep efficiency of a smaller spacing between the injection wells.

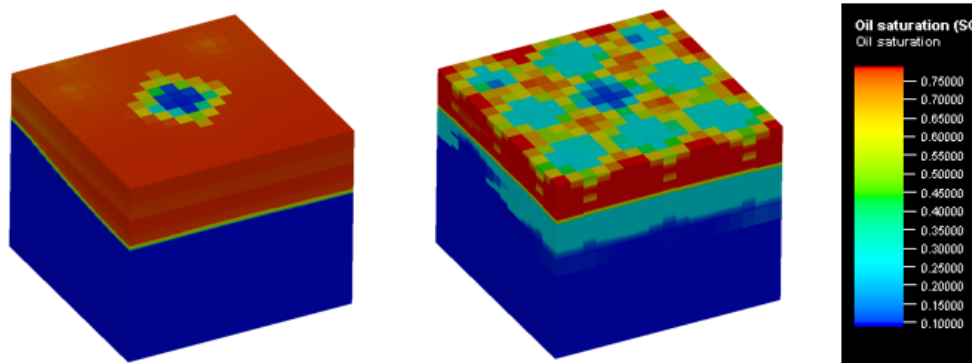


Figure 44: Block HIGH; oil saturation 2039, base case vs 5 spot pattern (inverted)

The ultimate recovery was again compared for different injection patterns. Figure 45 shows the simulated ultimate recovery factors. Again, the simulation was stopped as a water cut of 98% was reached or after 180 years of injection. Although the ultimate recovery for the 5-spot pattern with a large spacing of 1,5 km is quite high (58%) it has to be pointed out that it would take very long (around 160 years of injection time) to achieve this recovery factor. Therefore a smaller spacing is recommended in this region.

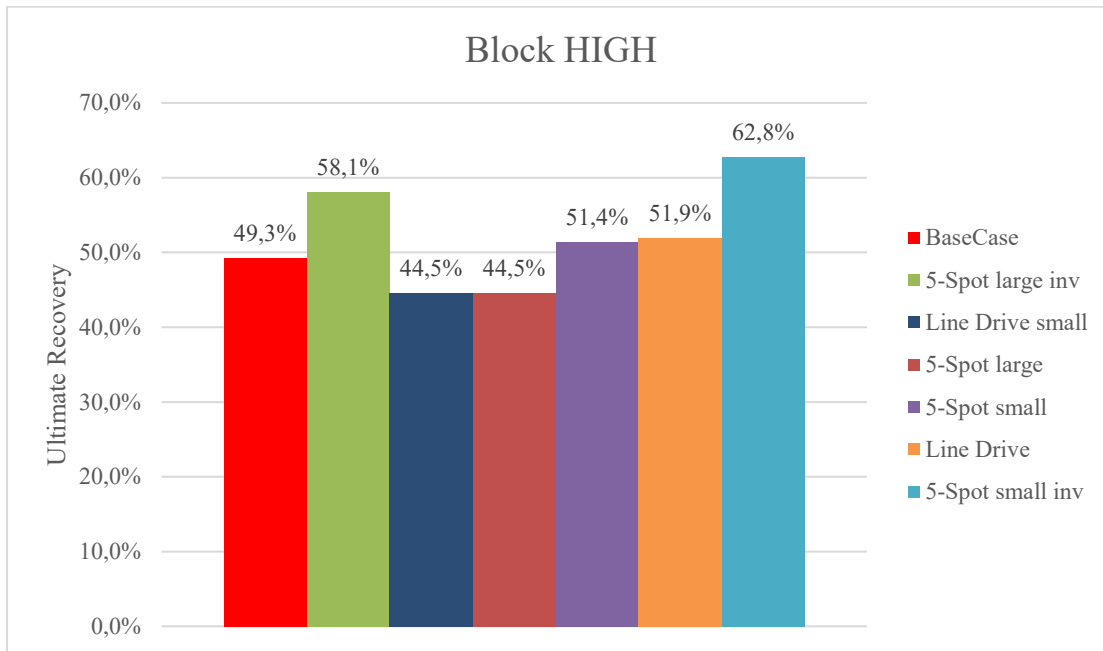


Figure 45: Block HIGH; ultimate recovery for different patterns

Taking the current well setting into account a new pattern was created to approach a 5-spot-pattern (inverted) with a smaller spacing. Additional injector wells are necessary. For the simulation four injector wells and two new producer wells were introduced. Figure 46 shows the current and the new injector/producer setting.

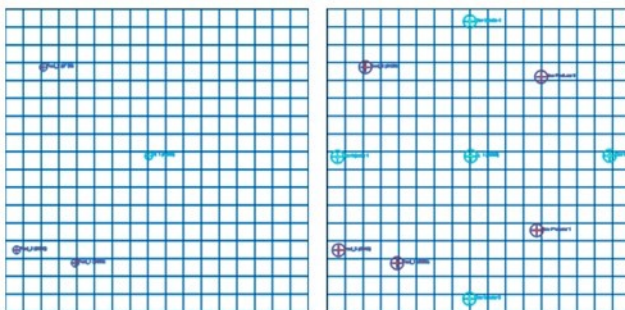


Figure 46: Block HIGH; base case and improved well setting

The recovery for the next 50 years was simulated. As visible in Figure 47 the recovery factor could be significantly improved (about 15%) by drilling the before mentioned additional wells.

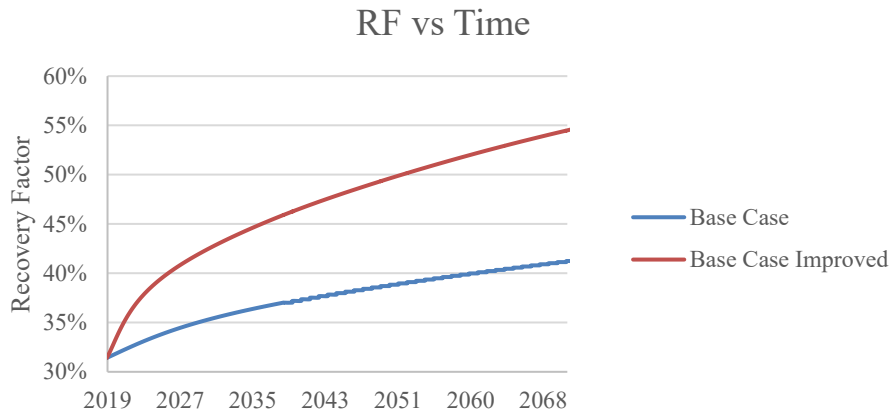


Figure 47: Block HIGH; recovery factor for improved well setting

Also looking at the oil saturation in 2039 shows the much better areal sweep efficiency for the improved well setting.

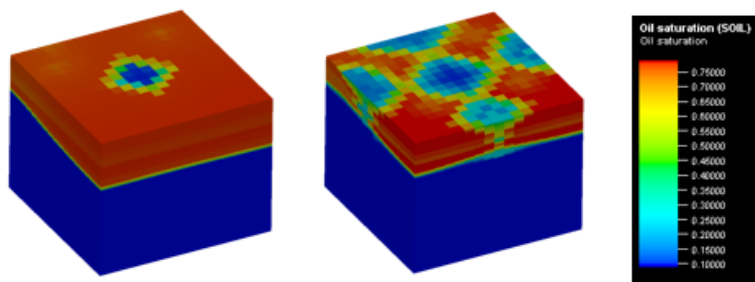


Figure 48: Block HIGH; oil saturation 2039; base case and improved base case

4.3 Block: Increasing

Also, for this block 3D properties porosity, initial water saturation and permeability from the exported sector and the homogeneous block model are visualized in Figure 49.

For the third block an area in the field was selected that does not perform very well according to the WOR Analysis. A block with currently two injectors and three producers was modelled. The spacing between two injectors is 1.4 km. The current field water cut is at 65%. The oil saturation of this block in 2019 is shown in Figure 50.

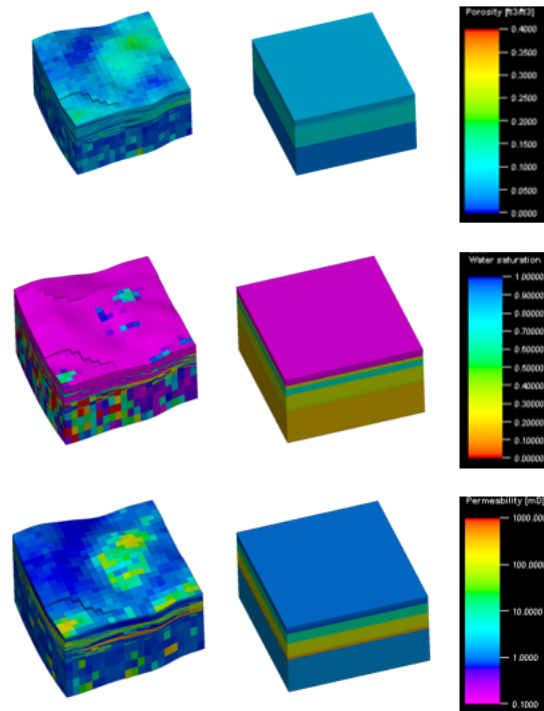


Figure 49: Block INCR; porosity (top), initial water saturation (middle) and permeability (bottom), exported sector and homogeneous block

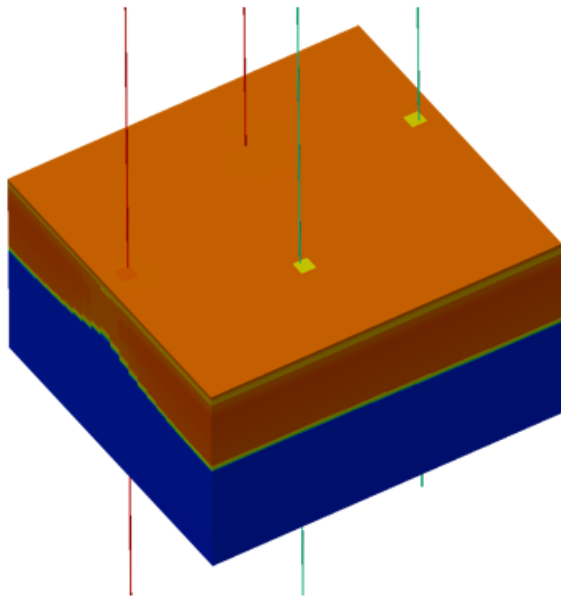


Figure 50: Block INCR; simulated oil saturation in 2019

This block shows the highest potential for increasing oil recovery by modifying the injection pattern. Figure 51 shows the possible recovery factors for different producer/injector settings. It is clearly visible that the current setting is quite insufficient in this region and modifications should be done to improve the recovery. Nearly all other settings led to an improved recovery. The best result could be achieved with a 5-spot-pattern with reduced spacing (750 m).

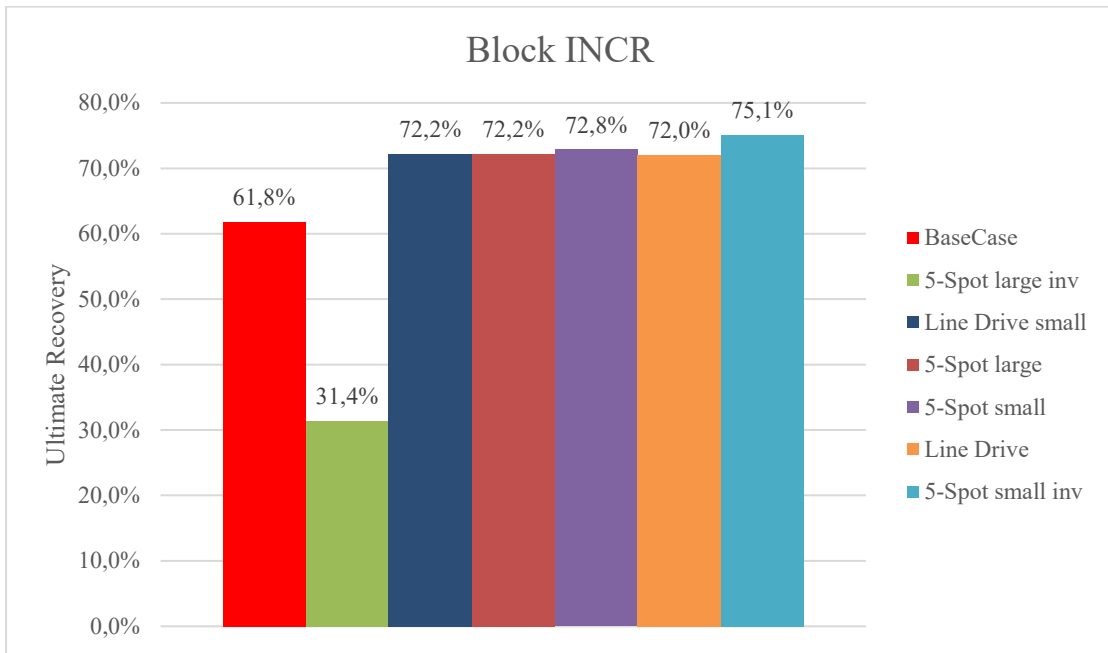


Figure 51: Block INCR; ultimate recovery for different patterns

When looking at the recovery factors in 2039 an additional recovery of up to 20% could be achieved by re-arranging the producer/injector pattern to a 5-spot-pattern with an injector-injector spacing of 750 m. The resulting oil saturation in 3D for the base case and the modified 5-spot injection pattern is shown in Figure 52.

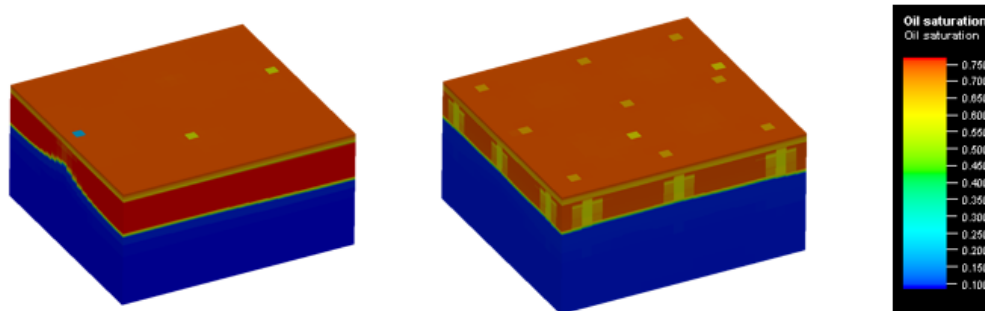


Figure 52: Block INCR: oil saturation 2039, base case vs 5 spot pattern

Nevertheless, changing the current well setting to a 5-spot-pattern with reduced spacing of 750m would lead to high costs and effort, as at least 9 new wells would be necessary. Also a larger spacing between the injector wells of 1.5 km still leads to a significantly improved recovery.

As a next step, the current well setting was investigated to find a proper improvement by drilling as few new wells as possible. As the 5-spot-pattern leads to the best result it was desired to create a well setting that represents that pattern.

In Figure 53 the simulated configuration is shown. Two new producers and three new injectors would be necessary. The recovery could be significantly improved. Within the next 50 years of production and injection a recovery of 81% could be achieved compared to a recovery of 60% for the current well setting.

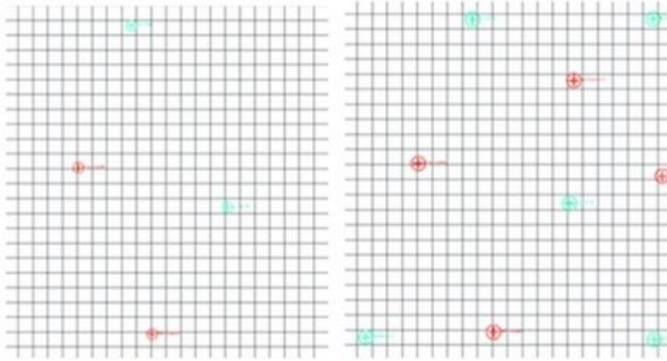


Figure 53: Block INCR; base case and improved well setting

Again, the recovery for the next 50 years was simulated. As visible Figure 54 the recovery factor could be improved by about 20% by drilling the additional wells.

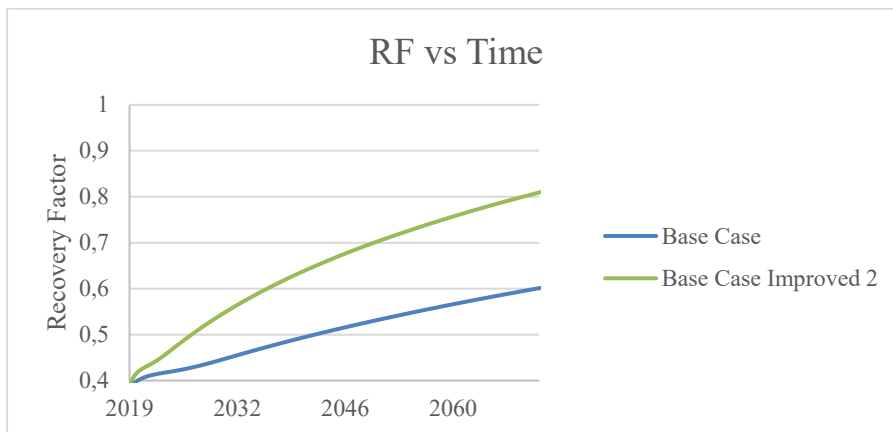


Figure 54: Block INCR; recovery factor for improved well setting

Also looking at the oil saturation in 2039 (Figure 55) reveals the beneficial effect of additional wells in this block.

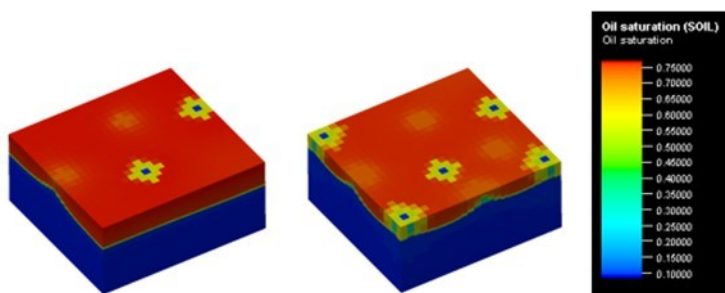


Figure 55: Block INCR; oil saturation 2039

4.4 Sector Models

The next step of the numerical simulation with Eclipse was to transfer the findings of the block modelling to a bigger scale. As mentioned, it was decided to not apply any changes in the “Low” pressure region, as the current well setting leads to a sufficient recovery efficiency. For the “High” and the “Increasing” pressure region modifications should be applied and the current injector setting should be transferred from a line-drive to a 5-spot pattern flood.

The simulation model including the history match was provided by OMV.

Several simulation runs were performed to reach a reasonable recovery with as little additional wells as possible. For the “High” pressure region, the whole region was considered for building a 5-spot-Pattern. For the “Increasing” pressure region only the part with low performance according to the WOR-analysis was considered for the pattern flood. The regions of interest are outlined in Figure 56.

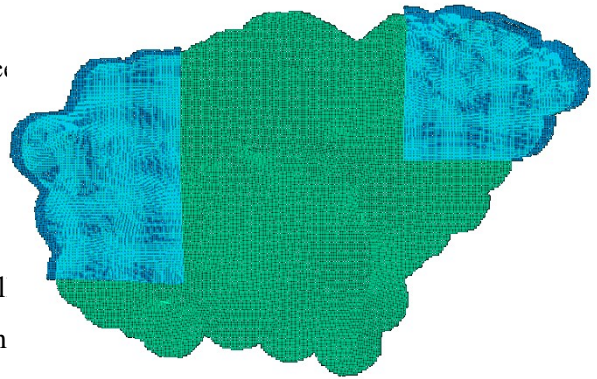


Figure 56: Regions for injection pattern modification

As a first run in both regions the current well setting (=base case) was simulated. Afterwards the spot-pattern with a spacing of around 1000m was tested. The oil saturation in 2019 was considered

to select proper locations for new producers and injectors. The oil production of all production wells was evaluated to exclude producers with low performance and to minimize the number of wells that have to be drilled. Also the corresponding injectors to these excluded producer wells were removed for the third simulation run. This step was repeated to find the optimum solution with a high recovery and a minimum number of new wells. For all simulation runs the water injection was controlled by rate (surface injection rate 4,500 STB/day) and the production was controlled by the bottomhole pressure (3,000 psi bottomhole pressure).

Only vertical producers and injectors were considered for the simulation. Due to technological hurdles and former issues with the drilling of horizontal wells, it was out of scope for this re-development plan to include horizontal wells in the simulation.

4.4.1 Pressure Region: High

In this region 16 producer wells and only 4 injection wells are currently active. Due to this very low number of injectors it was expected that a relatively high number of injection wells would be necessary to create a 5-spot injection pattern. In Figure 57 the current well setting is shown on the left side (producers=red, injectors=light blue). By the introduction of new injector and producer wells a 5-spot-pattern was approached (as shown on the right side). New injector wells are shown in dark blue and new production wells in orange. For this setting a total number of 35 new injectors and 17 new producers would be necessary.

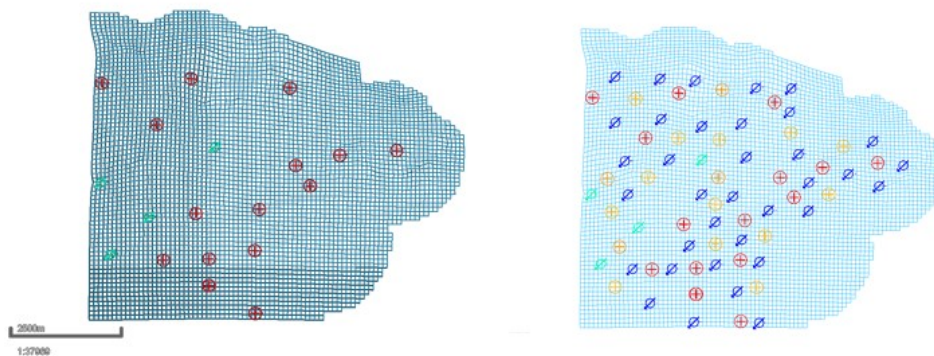


Figure 57: Pressure region HIGH; well setting base case vs 5-spot-pattern

The forecasted cumulative oil production could be doubled until 2045 (from 118.8 MMSTB to 242.9 MMSTB). Nevertheless, 52 new wells lead to huge investments and the well-by-well evaluation revealed some very low producing wells. Those production wells and their corresponding injection wells were excluded for the reduced case. The modified producer/injector-setting is shown in Figure 58 on the left side. For this setting 25 new injectors and 11 new producers are necessary. The cumulative oil production in 2045 is 232.7 MMSTB. Once again the production wells were evaluated to reduce the amount of necessary new wells. All producers that start with a production rate of less than 1,000 STB/day and their corresponding injection wells were excluded. Finally only 7 new producers and 16 new injectors were used to reach a cumulative production of 199.6 MMSTB in 2045.

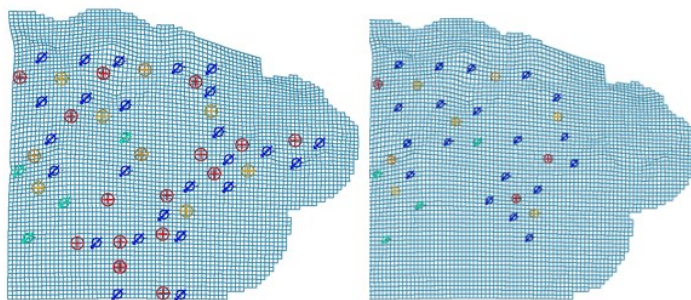


Figure 58: Pressure region HIGH; well setting reduced 1 & 2

The cumulative oil production for the four simulated runs is shown in Figure 59. “base case” represents the current well setting, “Improved” is the 5-spot-pattern with 52 new wells, “Improved_Reduced” shows the simulation case with 36 new wells and “Improved_Reduced_Reduced” visualizes the simulation with 23 new wells.

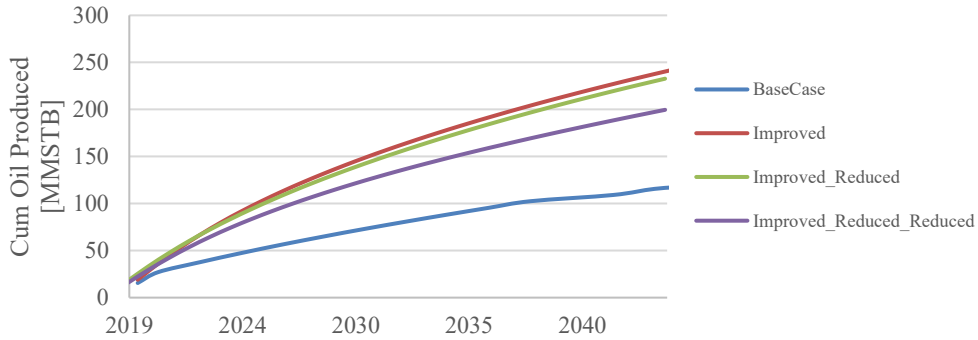


Figure 59: Pressure region HIGH; cum oil produced

Due to the additional number of injector wells apparently the volume of cumulatively injected water increased. Figure 60 shows the relation of the amount of injected water to the produced oil.

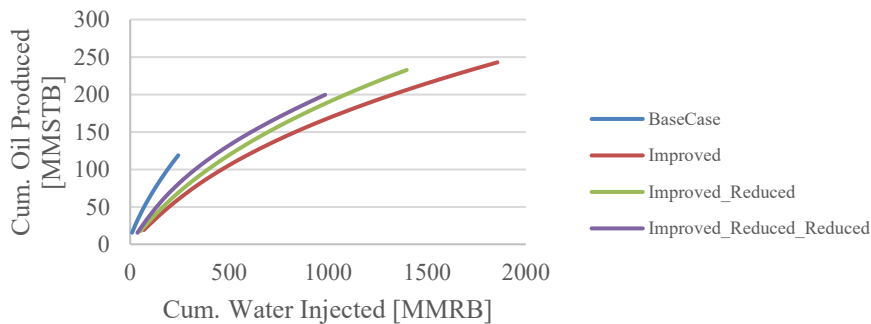


Figure 60: Pressure region HIGH; cum. oil produced vs. cum. water injected

Also looking at the saturation profile of this region reveals the beneficial effect of additional wells on the sweep efficiency. The first picture shows the current saturation of the field in 2019. All other saturation distributions are visualized after 20 years of production.

- Top left: saturation state in 2019
- Middle left: base case
- Middle right: improved (5-spot-pattern) with 52 new wells
- Bottom left: improved case with reduced number of wells (36 new wells)
- Bottom right: improved case with further reduced number of wells (23 new wells)

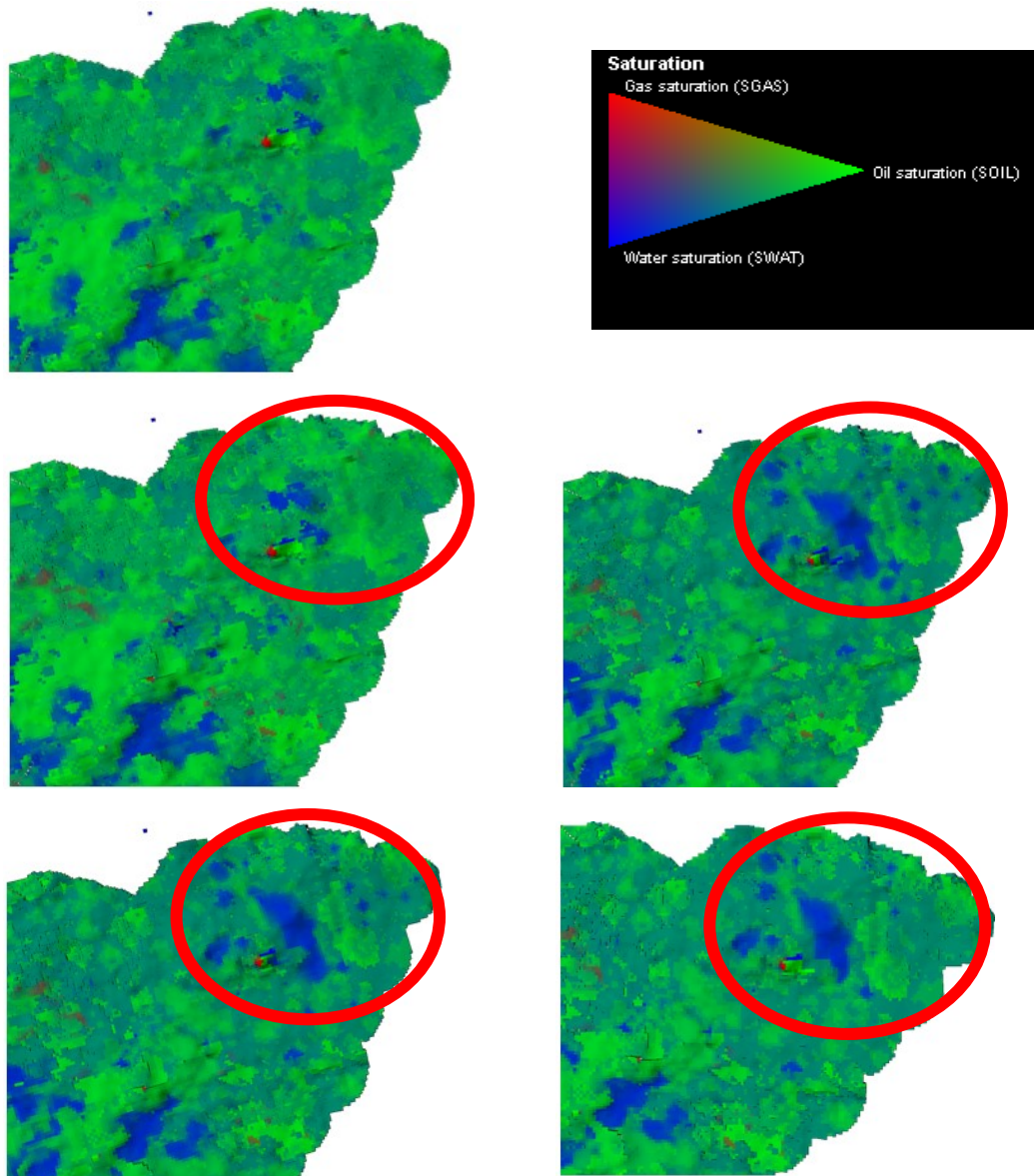


Figure 61: Pressure region HIGH; saturation profiles

4.4.2 Pressure Region: Increasing

In this region of the field 30 producers and 11 injectors are currently active. The WOR-analysis has shown that the currently installed line-drive-flood shows a rather poor performance. During the block modelling it was determined that a 5-spot pattern with a spacing of 800-1,500 m should lead to a significantly enhanced oil production. Therefore the current setting was modified to approach a 5-spot pattern. In Figure 62 the base case is shown on the left side. Again the currently active producers are shown in red and currently active injectors are shown in light blue. On the right side the pattern flood is visualized with new producers in orange and new injectors in dark blue. In total, 10 new producers and 44 new injectors were used. The cumulative production in 2045 could be enhanced from 121.3 MMSTB to 175.4 MMSTB.

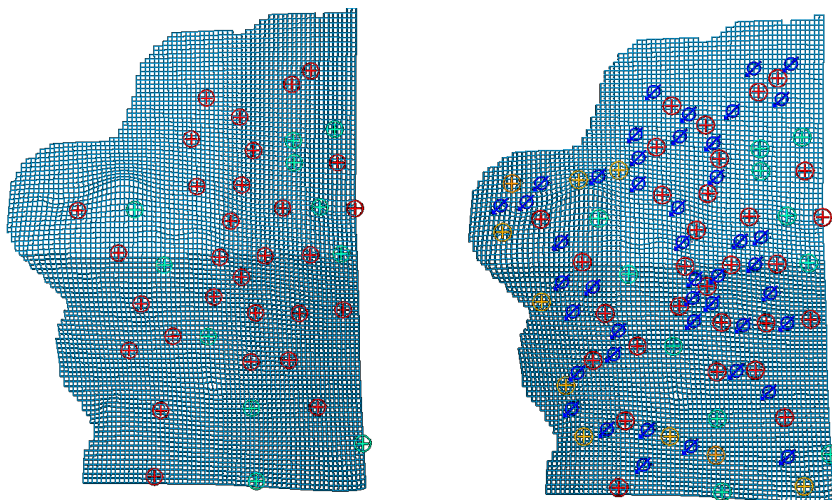


Figure 62: Pressure region INCR; well setting base case vs 5-spot-pattern

To again minimize the necessary amount of new wells a well-by-well-evaluation was performed, which led to the injector/producer setting shown in Figure 63. For this setting only 3 new producers and 21 new injectors are necessary. The cumulative production in 2045 only slightly decreased to 167.2 MMSTB.

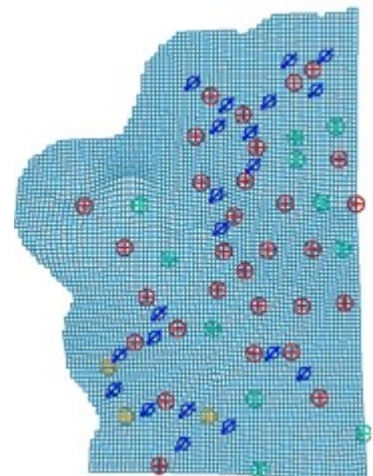


Figure 63: Pressure region INCR; 5-spot-pattern reduced

The cumulative oil production is summarized in Figure 64. “base case” describes the current well setting with 41 wells in total. “Improved” shows the 5-spot-pattern with additionally 54 wells and “Improved_Reduced” is the reduced 5-spot-pattern with only 24 new wells.

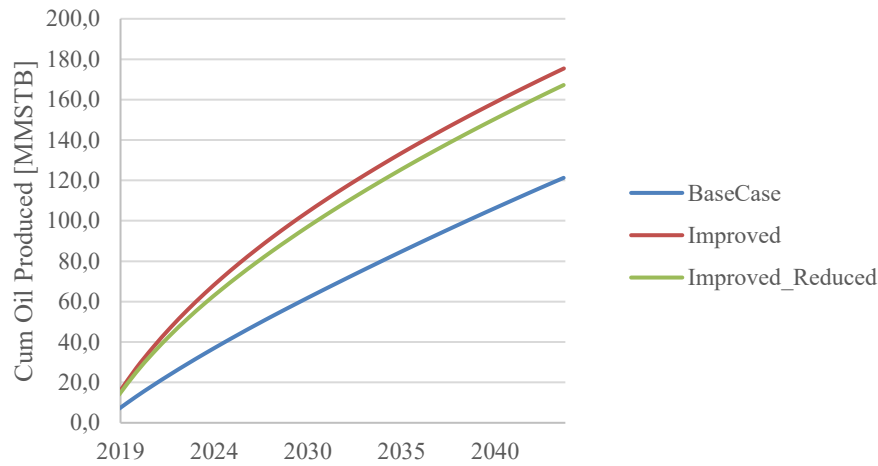


Figure 64: Pressure region INCR; cum. oil produced over time

By comparing the cumulative oil production with the cumulative water injection it can be determined that the reduced option of the 5-spot-pattern is more efficient, because less cumulative injected water leads to higher volumes of produced oil.

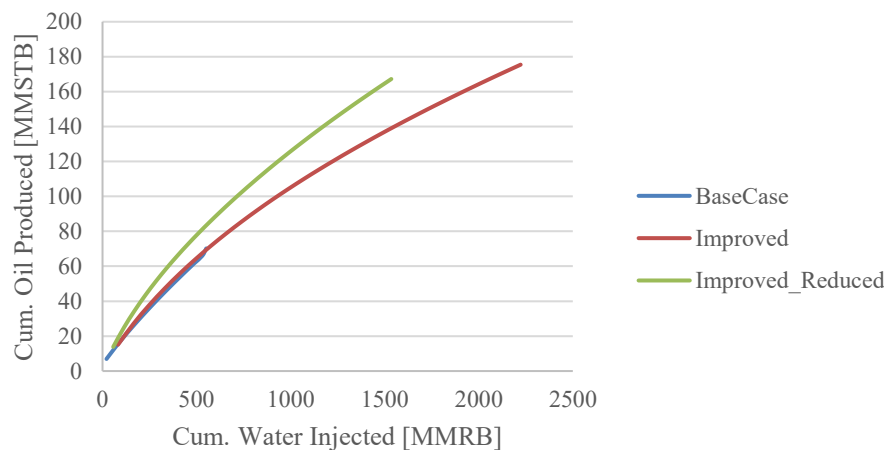


Figure 65: Pressure region INCR; cum. oil produced vs. cum. water injected

Looking at the saturation profile in 2045 (compared to 2019) shows the beneficial effect of additional wells in regards of the areal sweep efficiency:

- Top left: saturation profile in 2019
- Top right: base case 2045
- Bottom left: improved case (5-spot-pattern) 2045
- Bottom right: improved-reduced case (5-spot-pattern reduced) 2045

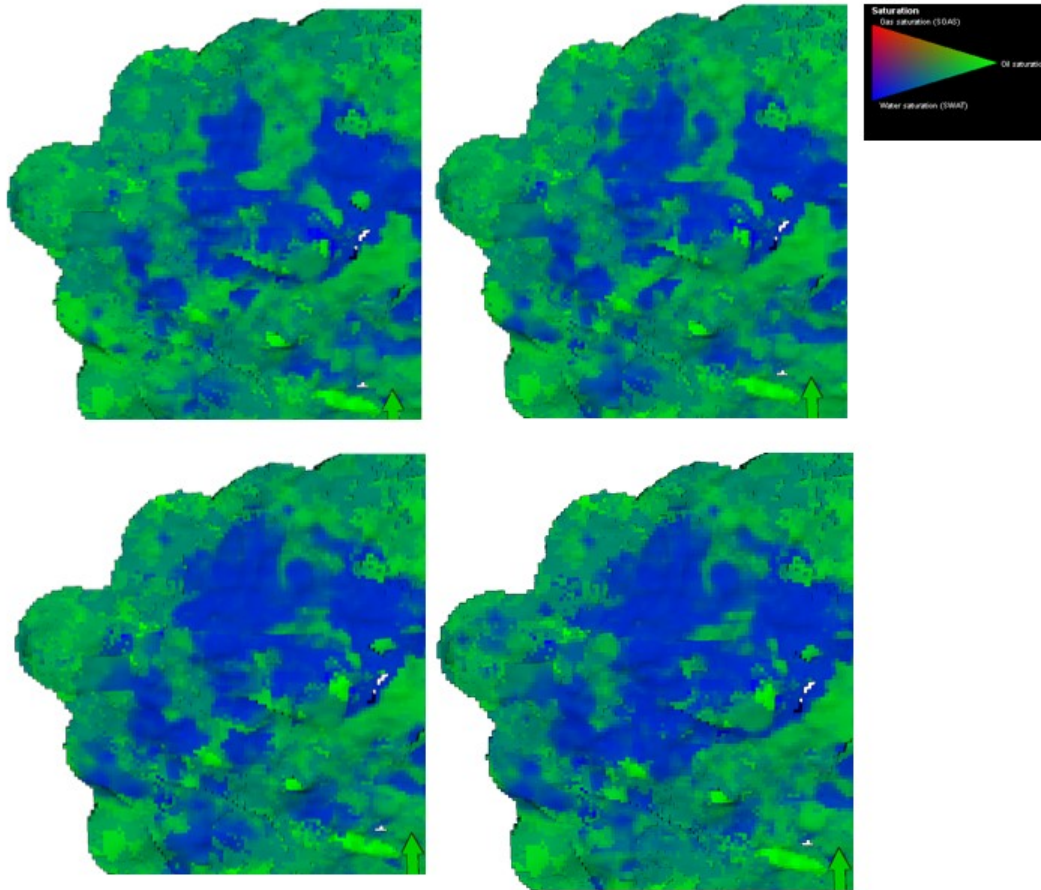


Figure 66: Pressure region INCR; saturation profiles

Chapter 5

Results and Discussion

A short economic calculation was performed to give the numerical results more expressiveness and to evaluate whether or not the additional wells should be drilled.

There are three drilling rigs available for the drilling of vertical wells. One well takes around 3 months to be drilled and completed. This means that every year it is possible to drill 12 new wells. As the re-development should be finished within 2 years, a maximum number of 24 wells can be drilled. Therefore only the reduced 5-spot-patterns for the “High” and “Increasing” pressure regions were considered for the economic evaluation.

Operational costs (OPEX) and capital expenditures (CAPEX) were provided by OMV. Total costs for a vertical producer are 7 MMUSD and for a vertical injector 6.7 MMUSD. Additionally, CAPEX of 2.3 USD/bbl and OPEX of 6.9 USD/bbl should be considered. Due to confidentiality agreements it is not possible to further clarify and split these costs.

A NPV (Net Present Value) calculation was performed for both sectors. The discount factor is 15%, according to OMV company rules. All incomes are discounted to 2019. Drilling and completion CAPEX are captured in 2019, 2020 and 2021.

5.1 Economic Evaluation Pressure Region “High”

In this region of the field 23 new wells (7 producers and 16 injectors) need to be drilled according to the numerical simulation. The comparison of CAPEX and oil production between the base case and the improved pattern is shown in Figure 67.

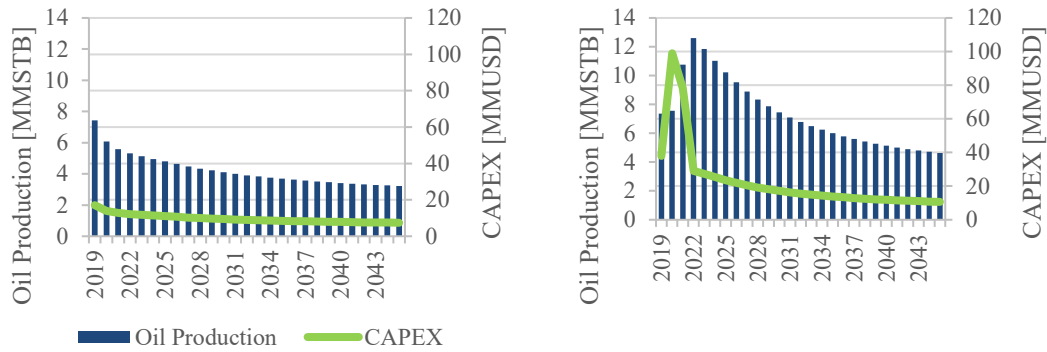


Figure 67: Sector HIGH; oil production and CAPEX base case vs. improved case

The NPV calculation emphasizes the importance of improving the production pattern. As shown in Figure 68 the NPV can be increased from 2.3 BUSD to 2.8 BUSD until 2045. The drilling of additional producers and injectors is therefore highly recommended.

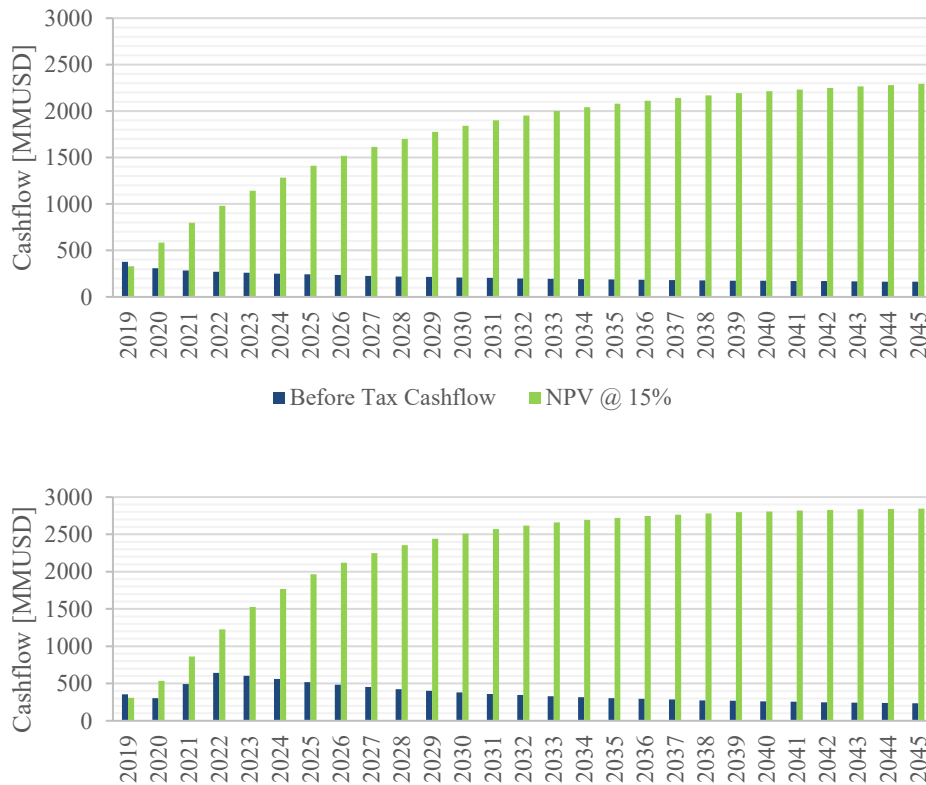


Figure 68: Sector HIGH; NPV and Before Tax Cashflow base case vs. improved case

5.2 Economic Evaluation Pressure Region “Increasing”

In the increasing pressure region it was determined that drilling 24 new wells leads to a significantly improved recovery. Also for this region CAPEX and oil production are compared in Figure 69.

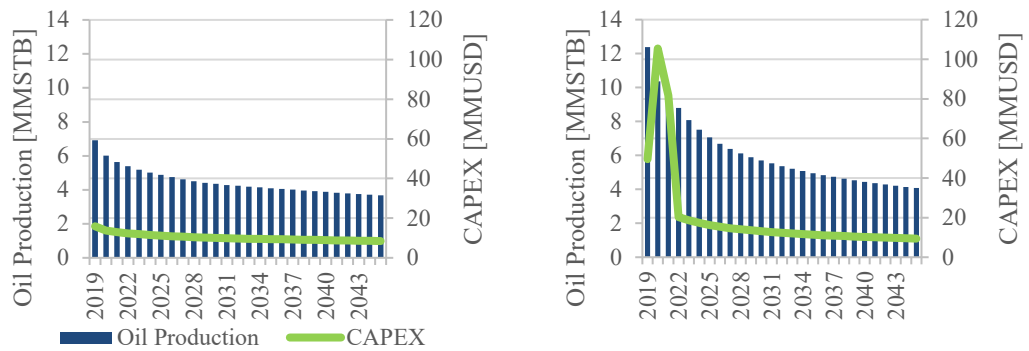


Figure 69: Sector INCR; oil production and CAPEX base case vs. improved case

In this case the Net Present Value could be enhanced from 1.7 BUSD to 2.6 BUSD, which again represents a significant improvement and therefore the drilling of additional wells is again highly recommended in this area.

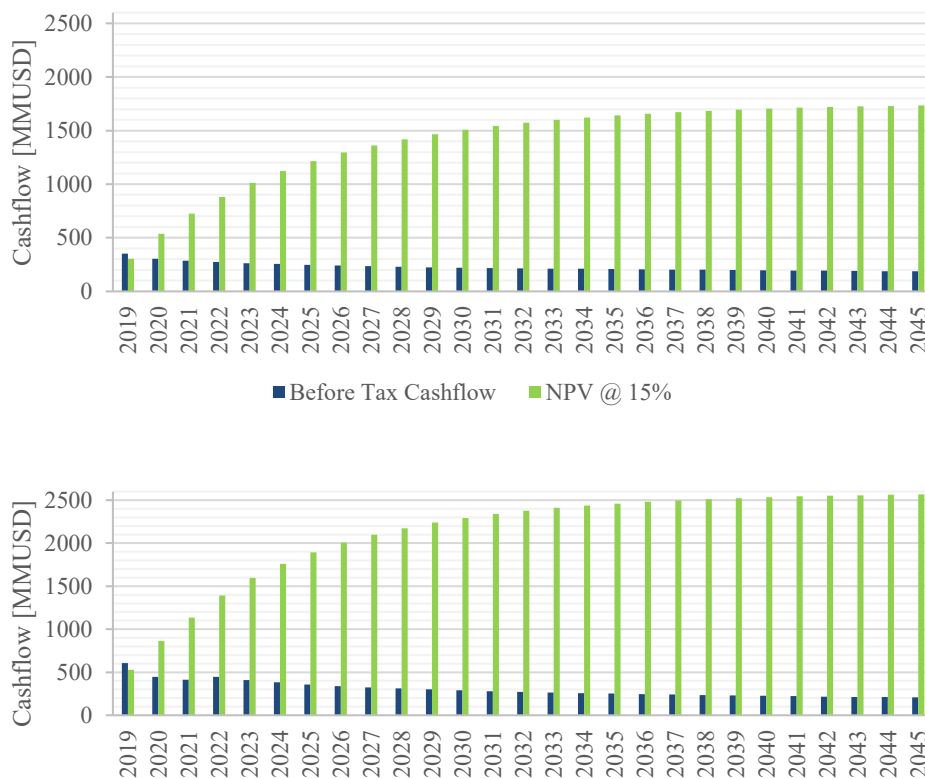


Figure 70: Sector INCR; NPV and Before Tax Cashflow base case vs. improved case

Chapter 6

Conclusion

6.1 Summary

The goal of this thesis was to support the OMV project team by the planning process of the re-development of a Libyan oil field in the Sirte Basin, which will take place in the next few years. The task was to provide another point of view and new ideas to improve the recovery efficiency of the whole field. Modifications of the injection scheme from line drive to pattern flood should be evaluated in different regions of the field. It is desired that new infill injectors and producers enhance the production performance of the field significantly.

Different types of analysis of analytical and numerical kind were performed. For the analysis historical pressure data, production and injection volumes and data from laboratory tests was provided by the operator. Furthermore a reservoir model in Petrel (including a reasonable history match) was available. No review of this model was performed, as this was out of scope of this thesis.

Several constraints and uncertainties needed to be taken into account. Afterwards, all results should be combined to find a best-possible prediction and based on that a well-founded recommendation for the well pattern modifications. Areas with insufficient production performance should be improved to enhance the efficiency of the waterflood. In the end an economical evaluation should proof that the recommended actions lead to substantial additional incomes.

Finally, the drilling of 47 new wells (10 production wells and 39 injection wells) was determined to lead to a remarkable increased cumulative oil production and net present value. The production could be enhanced from 240 MMSTB to 360 MMSTB until end of field life in 2045, which would lead to additional earnings of 1.4 BUSD.

6.2 Evaluation

Close consideration was given to all tasks that were specified in the scope of this thesis. Results were evaluated from different perspectives to reduce uncertainties as much as possible. Nevertheless, data quality was in some cases quite poor and assumptions were necessary for analytical and numerical predictions. The history match was provided and the examination was out of scope of this thesis. Also the verification of rock/physics functions and the PVT-fluid model were out of scope. Obviously, possible errors in this data could highly influence the results and might lead to wrong predictions. To find a transition between analytical and numerical results first MBAL was used, which works with material balance equations to match historical pressure and production data. Although this analysis could help to identify drive mechanisms and predict the future performance of the field, the application is highly limited and estimations should only act as a very rough guideline. Nevertheless, this simulation revealed a possible error in the estimation of oil initially in place, which might be too optimistic. Further analysis should be performed to check the veracity of this result. The homogenous block models created with Petrel were useful as a first-look interpretation of different well settings and to evaluate the performance of various well spacings. The simulations revealed some surprisingly high improvement potentials by re-arranging the well pattern and drilling additional injectors and producers. However, no structural features at all were considered in those blocks and the regarded oil field is highly heterogeneous with numerous faults. These circumstances clearly indicate that the results of this block models are questionable to some degree and should be considered with caution.

Despite everything, the application of those results of the block modelling process also worked out quite well on the full field reservoir model and finally the cumulative oil production could be enhanced considerably with the recommended infill producers and injectors.

Simple, homogeneous block models provide very useful insights with comparably low effort. Especially for projects with limited data and insufficient information about geological features (folds, faults etc.) this approach can be applied to gain useful ideas for the enhancement of recovery efficiency. On the other hand, for reservoirs that are dominated by effects from geological features or varying petrophysical properties, the applicability of homogeneous block models is obviously highly limited. Therefore, engineers should decide as the case arises, if the application of homogeneous block models provides useful information or if results might be too misleading and no additional valuable insights can be gained.

6.3 Future Work

To improve the significance of the results it would be better to present a range of possible outcomes with corresponding probabilities. Improvements on the reliability of the predictions could be realized by applying “stochastic modelling workflow”. Simulations are performed on a set of several hundred conceivably geological models with different property distributions (initial water saturation, porosity, horizontal and vertical permeability etc.). Those “ranges of possible outcomes” will highly improve the expressiveness of the results as no single values, but ranges of potential results are much more likely to predict the future production in a meaningful way. Applying the recommended re-development strategy with the new drilling locations to such a process should be done in future to evaluate the enhancement on the recovery efficiency of the field.

OMV acts as non-operator in this project. A comprehensive field development plan, including actions of several disciplines will be compiled and presented in a target meeting with all project partners. At this meeting several possibilities will be discussed with the operating oil company and decisions about future actions will be taken.

Chapter 7

References

- Anon., 2012. *Fekete.com*. [Online] Available at: http://fekete.com/SAN/TheoryAndEquations/HarmonyTheoryEquations/Content/HTML_Files/Reference_Material/Analysis_Method_Theory/Surveillance_Theory.htm [Zugriff am 19 02 2019].
- Bailey, B. et al., 2000. *Schlumberger Oil Field Review on Water Control*. s.l.:Spring.
- Bradley, H. B., 1987. *Petroleum Engineering Handbook*. United States of America: Richardson, TX, Society of Petroleum Engineers.
- Buckley, S. E. & Leverett, M. C., 1942. Mechanism of Fluid Displacement in Sands. *Transactions of the AIME*, 146(01), pp. 107-116.
- Cobb, W. M. & Marek, F. J., 1997. Determination of Volumetric Sweep Efficiency in Matura Waterfloods Using Production Data. *SPE 38902*, 22(2), pp. 93-100.
- Cole, F., 1969. *Reservoir Engineering Manual*. Houston: Gulf Publishing Company.
- Craig, F. F., 1971. *The Reservoir Engineering Aspects of Waterflooding*. New York, Dallas: Society of Petroleum Engineers of AIME.
- Crawford, P. B., 1960. Factors Affecting Waterflood Pattern Performance and Selection. *Journal of Petroleum Technology*, 12(12), pp. 11-15.
- Dake, L. P., 1978. *Fundamentals of Reservoir Engineering*. The Hague: Elsevier.
- Deppe, J. C., 1961. Injection Rates - The Effect of Mobility Ratio, Area Swept, and Pattern. *SPE-1472-G*, 1(02), p. 11.

Dykstra, H. & Parsons, R. L., 1950. The Prediction of Oil Recovery by Waterflood. *Secondary Recovery of Oil in the United States, API*.

Emad Walid Al Shalabi & Kamy Sepehrnoori, 2017. *Low Salinity and Engineered Water Injection for Sandstone and Carbonate*. s.l.:Gulf Professional Publishing.

Feigl, A., 2011. Effect of trapped gas saturation on oil recovery during the application of secondary recovery methods in exploitation of petroleum reservoirs. *NAFTA*, pp. 153-159.

Kimbler, O. K., Caudle, B. H. & Cooper, H. E., 1964. Areal Sweepout Behavior in a Nine-Spot Injection Pattern. *Journal of Petroleum Technology*, 02(16), pp. 199-202.

Kleppe, J. & Skjæveland, S. M., 1992. *SPOR Monograph - Recent Advantages in Improved Oil Recovery Methods for North Sea Sandstone Reservoirs*. Stavanger: Norwegian Petroleum Directorate.

Lake, L. W., 2007. *Petroleum engineering handbook*. Richardson, TX: Society of Petroleum Engineers.

Mahani, H. et al., 2015. Kinetics of Low-Salinity-Flooding Effect. *SPE Journal*, 20(01), pp. 008-020.

Mehran, S., Masoud, R., Mahmoud, J. & Nor, I., 2011. *Carbonated water injection (CWI)–A productive way of using CO₂ for oil recovery and CO₂ storage*. s.l.:Elsevier.

Muchitsch, M. & Kratzer, D., 2005. *Nafloor Augila Unit - Reservoir Simulation Study*, Leoben: Hot Engineering GmbH.

Muskat, M., 1951. Physical Principles of Oil Production. *The Journal of Geology*, 59(5), pp. 513-515.

Nnaemeka, E., 2010. *Petroleum Reservoir Engineering Practice*. Boston, MA: Pearson Education, Inc..

OMV, O. A., 2008. *Improved Oil Recovery Development Plan*, s.l.: OMV, Oxy, Agoco.

Rose, S. C., Buckwalter, J. F. & Woodhall, R. J., 1989. *The Design Engineering Aspects of Waterflooding*. Richardson, Texas: Monograph Series, SPE.

Stiles, W. E., 1949. Use of Permeability Distribution in Water-flood Calculations. *Journal of Petroleum Technology*, 1(01), pp. 9-13.

Thakur, G. C., 1998. The Role of Reservoir Management in Carbonate Waterfloods. *Journal of Petroleum Technology*, 50(12), pp. 62-63.

Walsh, M., 1995. A Generalized Approach to Reservoir Material Balance Calculations. *Journal of Canadian Petroleum Technology*, 34(01).

Welge, H. J., 1952. A Simplified Method for Computing Oil Recoveries by Gas or Water Drive. *Journal of Petroleum Technology*, 4(04), pp. 91-98.

List of Figures

Figure 1: Index map (OMV, 2008).....	13
Figure 2: Cross section across Sirte Basin (OMV, 2008).....	14
Figure 3: Lithostratigraphic Column (Muchitsch & Kratzer, 2005).....	14
Figure 4: Water injectivity variation (Craig, 1971).....	18
Figure 5: Common waterflood-pattern configurations (Rose, et al., 1989).....	22
Figure 6: Instantaneous VRR and cumulative VRR for a sample set of wells (Anon., 2012).24	
Figure 7: Schematic capillary desaturation curve (Kleppe & Skjæveland, 1992).....	34
Figure 8: PVT properties.....	37
Figure 9: Pressure Analysis, raw and cleaned data.....	38
Figure 10: Different pressure regions (green=LOW; blue=HIGH; red=INCR).....	39
Figure 11: Pressure regions.....	39
Figure 12: WOR whole field.....	40
Figure 13: Division of the field into sectors.....	40
Figure 14: WOR of individual blocks.....	41
Figure 15: Water cut analysis.....	42
Figure 16: Analytically derived vertical sweep efficiency.....	43
Figure 17: Injection line for BL analysis.....	44
Figure 18: Rel. permeabilities and fractional flow curves layers F, G and H.....	45
Figure 19: BL profile for injection line.....	46
Figure 20: BL profile for G-073.....	46
Figure 21: Oil production, water production & injection, pressure on field basis.....	47
Figure 22: Oil production, water production & injection, pressure for pressure regions.....	48
Figure 23: MBAL – full field simulation, original.....	48
Figure 24: MBAL – full field simulation, adjusted injection rates.....	49
Figure 25: MBAL – full field simulation, adjusted OOIP.....	49
Figure 26: MBAL model - multitank.....	50
Figure 27: MBAL – pressure regions, original data.....	50
Figure 28: MBAL – pressure regions, adjusted injection rates.....	51
Figure 29: Comparison of water injection modifications.....	51
Figure 30: MBAL model - multitank extended.....	52
Figure 31: MBAL – pressure regions, loss zones and aquifer.....	52
Figure 32: MBAL – pressure regions, aquifer influx.....	53
Figure 33: MBAL – pressure regions, cumulative oil production.....	53
Figure 34: Well settings 5 spot large/small spacing, line drive large/small spacing.....	55
Figure 35: Location of blocks (green=increasing; yellow=high; red=low).....	56
Figure 36: Block LOW; exported block and homogeneous sector model (porosity).....	57
Figure 37: Block LOW; comparison homogeneous block to exported sector.....	57
Figure 38: Block LOW; porosity (top), initial water saturation (middle) and permeability (bottom), exported sector and homogeneous block.....	58
Figure 39: Block LOW; simulated oil saturation in 2019.....	59
Figure 40: Block LOW; oil saturation 1 PV injected, base case vs 5 spot pattern.....	59
Figure 41: Block LOW; Ultimate Recovery for different Patterns.....	60
Figure 42: Block HIGH; porosity (top), initial water saturation (middle) and permeability (bottom), exported sector and homogeneous block.....	60
Figure 43: Block HIGH; simulated oil saturation in 2019.....	61
Figure 44: Block HIGH; oil saturation 2039, base case vs 5 spot pattern (inverted).....	61
Figure 45: Block HIGH; ultimate recovery for different patterns.....	62
Figure 46: Block HIGH; base case and improved well setting.....	62
Figure 47: Block HIGH; recovery factor for improved well setting.....	63
Figure 48: Block HIGH; oil saturation 2039; base case and improved base case.....	63

Figure 49: Block INCR; porosity (top), initial water saturation (middle) and permeability (bottom), exported sector and homogeneous block	64
Figure 50: Block INCR; simulated oil saturation in 2019	64
Figure 51: Block INCR; ultimate recovery for different patterns.....	65
Figure 52: Block INCR; oil saturation 2039, base case vs 5 spot pattern.....	65
Figure 53: Block INCR; base case and improved well setting	66
Figure 54: Block INCR; recovery factor for improved well setting	66
Figure 55: Block INCR; oil saturation 2039	66
Figure 56: Regions for injection pattern modification.....	67
Figure 57: Pressure region HIGH; well setting base case vs 5-spot-pattern.....	68
Figure 58: Pressure region HIGH; well setting reduced 1 & 2	68
Figure 59: Pressure region HIGH; cum oil produced	69
Figure 60: Pressure region HIGH; cum. oil produced vs. cum. water injected	69
Figure 61: Pressure region HIGH; saturation profiles	70
Figure 62: Pressure region INCR; well setting base case vs 5-spot-pattern	71
Figure 63: Pressure region INCR; 5-spot-pattern reduced.....	71
Figure 64: Pressure region INCR; cum. oil produced over time.....	72
Figure 65: Pressure region INCR; cum. oil produced vs. cum. water injected.....	72
Figure 66: Pressure region INCR; saturation profiles.....	73
Figure 67: Sector HIGH; oil production and CAPEX base case vs. improved case.....	76
Figure 68: Sector HIGH; NPV and Before Tax Cashflow base case vs. improved case	76
Figure 69: Sector INCR; oil production and CAPEX base case vs. improved case	77
Figure 70: Sector INCR; NPV and Before Tax Cashflow base case vs. improved case	77

Nomenclature

A	Area	[m ²]
B_g	Formation Volume Factor Gas	[rcf/scf]
B_o	Formation Volume Factor Oil	[rbbl/STB]
B_w	Formation Volume Factor Water	[rbbl/STB]
F_w	Fractional flow of water	[-]
E	Overall Displacement Efficiency	[-]
E_A	Volumetric Areal Sweep Efficiency	[-]
E_D	Displacement Efficiency	[-]
E_v	Volumetric Sweep Efficiency	[-]
E_L	Volumetric Length Sweep Efficiency	[-]
i	Injectivity	[bbl/psi]
k	Permeability	[mD]
M	Mobility Ratio	[-]
N	Initial Oil Volume	[bbl]
N_d	oil displaced from the swept parts of the reservoir	
N_p	Volume Oil Produced	[bbl]
R_s	Solution Gas Oil Ratio	[scf/bbl]
S_{oi}	Initial Oil Saturation	[-]
S_{wi}	Initial Water Saturation	[-]
S_{wirr}	Irreducible Water Saturation	[-]
S_{wc}	Connate Water Saturation	[-]
Q	Rate	[bbl]
V_p	Pore Volume	[-]
μ	Viscosity	[cp]
ρ	Density	[kg/m ³]

Φ

Porosity

[-]

Abbreviations

Approx.	approximately
BOPD	Barrels Oil Per Day
BUSD	Billion USD
Cum.	Cumulative
GOR	Gas Oil Ratio
INCR	Increasing
M	Mobility Ratio
MMSTB	Million Stock Tank Barrels
mPas	Milli-Pascal-Sekunden
P	Pressure
Rbbl	Reservoir barrel
RF	Recovery Factor
VRR	Voidage Replacement Ratio
WC	Water Cut
WOR	Water Oil Ratio